

(Tri-*tert*-butylsilyl)imido Complexes of Titanium: Benzene C–H Activation and Structure of [(^tBu₃SiNH)Ti]₂(μ-NSi^tBu₃)₂Christopher C. Cummins, Christopher P. Schaller, Gregory D. Van Duyne, Peter T. Wolczanski,*[†] A. W. Edith Chan, and Roald Hoffmann

Contribution from the Department of Chemistry, Baker Laboratory, Cornell University, Ithaca, New York 14853. Received August 6, 1990

Abstract: Treatment of TiCl₄(THF)₂ with 3.0 equiv of ^tBu₃SiNHLi in Et₂O produced (^tBu₃SiNH)₃TiCl (**1**; 82%). An attempt to alkylate **1** with MeMgBr led to (^tBu₃SiNH)₃TiBr (**2**), alternatively prepared from **1** and MgBr₂ (41%), and addition of MeLi to **1** yielded (^tBu₃SiNH)₂(Et₂O)Ti=NSi^tBu₃ (**4**; 55%) and CH₄ via dehydrochlorination and Et₂O trapping of transient [(^tBu₃SiNH)₂Ti=NSi^tBu₃] (**3**). The amido protons of **4** are deuterated through addition/elimination of a benzene-*d*₆ C–D bond to the imido ligand of transient **3**. A similar deuteration of **1**, **2**, and (^tBu₃SiNH)₄Ti (**12**) in C₆D₆ occurs via other reactive intermediates, [(^tBu₃SiNH)XTi=NSi^tBu₃] (X = Cl (**7**), Br (**8**), ^tBu₃SiNH (**3**)), produced by loss of ^tBu₃SiNH₂. Thermolysis of **1**, **2**, and **12** in C₆D₆/THF or THF afforded (^tBu₃SiNH)(THF)XTi=NSi^tBu₃ (X = Cl (**9**), Br (**11**), ^tBu₃SiNH (**13**)) and ^tBu₃SiNH₂. Kinetic studies in C₆D₆/THF-*d*₈ revealed that formation of **9** is THF independent, amine elimination is rate determining ($k = 1.03 (1) \times 10^{-4} \text{ s}^{-1}$ at 80.5 °C; $\Delta H^\ddagger = 23.3 (8) \text{ kcal/mol}$, $\Delta S^\ddagger = -11 (2) \text{ eu}$; $k(\text{NH})_3/k(\text{ND})_3 = 5.9 (6)$ at 90.4 °C), and the rate of ^tBu₃SiNH₂ loss increases 10-fold when **12** is thermolyzed, consistent with an amide abstraction mechanism. Alkylation of **9** with MeLi or ^tBuLi provided (^tBu₃SiNH)(THF)RTi=NSi^tBu₃ (R = Me (**15**), 55%; ^tBu (**16**), 76%), respectively. Hydrogenation of either produced [(^tBu₃SiNH)Ti]₂(μ-NSi^tBu₃)₂ (**17**; 61% (97% by ¹H NMR)) through dimerization of transient hydride [(^tBu₃SiNH)(THF)HTi=NSi^tBu₃] (**18**), generated via σ-bond metathesis of Ti–R, according to labeling experiments. Crystal data for **17**: monoclinic, *P*2₁/*n*, *a* = 12.033 (3) Å, *b* = 23.309 (5) Å, *c* = 22.741 (4) Å, β = 99.314 (15)°, *V* = 6294 (2) Å³, *Z* = 4, *T* = –80 °C, *R* = 6.64%, *R*_w = 7.75% (7806 reflections where $|F_o| \geq 4\sigma(F_o)$). Dimer **17** has an unusual C₂ structure with an extremely short Ti–Ti bond (2.442 (1) Å) and titanium atoms 0.58 and 0.60 Å exo to their respective amido and both μ-NSi^tBu₃ ligands. EHMO calculations of **17** rationalize this geometry in terms of constraints imposed by the bridges and a single Ti–Ti bond of mixed composition.

Introduction

Organotransition-metal complexes possessing a degree of coordinative unsaturation are inherently reactive; consequently, investigations of these compounds provide a fundamental understanding of important bond-making and -breaking transformations.¹ Attack by various substrate molecules leads to adducts, bond activations, and the formation of dinuclear or multinuclear complexes,² some which contain metal–metal bonds.^{3,4} In these laboratories, coordinatively unsaturated early-transition-metal complexes have been generated through the use of bulky alkoxide, siloxide, and silamide ligands (e.g., ^tBu₃CO[–] (tritox),⁵ ^tBu₃SiO[–] (silox),^{6–9} and ^tBu₃SiNH[–]).^{10,11} Unusual η²-pyridine, η²-benzene,⁶ and ketyl⁷ adducts have been characterized, activations of molecular oxygen,⁵ carbon monoxide,^{8–10} and carbon–hydrogen bonds¹¹ have been explored, and unbridged binuclear hydride complexes, [(silox)₂MH₂]₂ (M = Nb, Ta),⁹ have been synthesized.

Recently, thermolyses of (^tBu₃SiNH)₃ZrR complexes were shown to generate a highly reactive transient, (^tBu₃SiNH)₂Zr=NSi^tBu₃, capable of carbon–hydrogen bond activation.¹¹ The capture of alkanes by the electrophilic, three-coordinate d⁰ zirconium center, in particular the subsequent addition of RH to the Zr=NSi^tBu₃ functionality, may be relevant to the oxidation of hydrocarbons by metal oxides,¹² since imido and oxo^{13,14} groups are isoelectronic. Formation of the imide occurred by a rate-determining abstraction^{15,16} of an amido hydrogen by the leaving alkyl, in accord with similar studies pertaining to RH elimination from Cp₂Zr(R)NHR' by Walsh and Bergman et al.¹⁷ In an effort to generate stable, low-coordinate, monomeric imido complexes, studies of analogous titanium derivatives were initiated in view of the smaller covalent radius of Ti (1.32 Å) relative to zirconium (1.45 Å). There exists a paucity of terminal imido species¹⁸ bound to titanium, with only Rothwell's (O-2,6-ⁱPr₂C₆H₃)₂(4-pyrrolidinopyridine)Ti=NP¹⁹ and Roesky's (py)₃Cl₂Ti=NP(S)Ph₂²⁰ structurally characterized. Through reactions best interpreted as amide abstractions, a series of titanium imido complexes has been prepared and their formation mechanistically evaluated. Included in this study are structural and theoretical

analyses of a binuclear comprising "(^tBu₃SiNH)Ti(NSi^tBu₃)" moieties, one that contains an extremely short Ti–Ti bond.

- (1) Parshall, G. W. *Homogeneous Catalysis*; Wiley: New York, 1980.
- (2) (a) Kochi, J. K. *Organometallic Mechanisms and Catalysis*; Academic: New York, 1978. (b) Collman, J. P.; Hegedus, L. S.; Norton, J. R.; Finke, R. G. *Principles and Applications of Organotransition Metal Chemistry*; University Science: Mill Valley, CA, 1987.
- (3) Messerle, L. *Chem. Rev.* **1989**, *89*, 1229–1254.
- (4) (a) Cotton, F. A.; Walton, R. A. *Multiple Bonds Between Metal Atoms*; Wiley: New York, 1982. (b) *Reactivity of Metal–Metal Bonds*; Chisholm, M. H., Ed.; Advances in Chemistry 155; American Chemical Society: Washington, DC, 1981.
- (5) Lubben, T. V.; Wolczanski, P. T. *J. Am. Chem. Soc.* **1987**, *109*, 424–435.
- (6) Neithamer, D. R.; Párkányi, L.; Mitchell, J. F.; Wolczanski, P. T. *J. Am. Chem. Soc.* **1988**, *110*, 4421–4423.
- (7) Covert, K. J.; Wolczanski, P. T. *Inorg. Chem.* **1989**, *28*, 4565–4567.
- (8) Neithamer, D. R.; LaPointe, R. E.; Wheeler, R. A.; Richeson, D. S.; Van Duyne, G. D.; Wolczanski, P. T. *J. Am. Chem. Soc.* **1989**, *111*, 9056–9072.
- (9) (a) Toreki, R.; LaPointe, R. E.; Wolczanski, P. T. *J. Am. Chem. Soc.* **1987**, *109*, 7558–7560. (b) LaPointe, R. E.; Wolczanski, P. T. *J. Am. Chem. Soc.* **1986**, *108*, 3535–3537.
- (10) Cummins, C. C.; Van Duyne, G. D.; Schaller, C. P.; Wolczanski, P. T. *Organometallics* **1991**, *10*, 164–170.
- (11) Cummins, C. C.; Baxter, S. M.; Wolczanski, P. T. *J. Am. Chem. Soc.* **1988**, *110*, 8731–8733. Details of the C–H activation chemistry will be published in due course: Cummins, C. C.; Schaller, C. P.; Wolczanski, P. T., unpublished results.
- (12) (a) Labinger, J. A.; Ott, K. *J. Phys. Chem.* **1987**, *91*, 2682–2684. (b) Sofranko, J. A.; Leonard, J. J.; Jones, C. A. *J. Catal.* **1987**, *103*, 302–310. (c) Tong, Y.; Rosynek, M. P.; Lunsford, J. H. *J. Phys. Chem.* **1989**, *93*, 2896–2898. (d) Campbell, K. D.; Morales, E.; Lunsford, J. H. *J. Am. Chem. Soc.* **1987**, *109*, 7900–7903. (e) Ekstrom, A.; Lapszewicz, J. A. *J. Am. Chem. Soc.* **1988**, *110*, 5226–5228. (f) Grasselli, R. K.; Burrington, J. D. *Adv. Catal.* **1981**, *30*, 133–163. (g) Burrington, J. D.; Kartisek, C. T.; Grasselli, R. K. *J. Catal.* **1983**, *81*, 489–498; **1984**, *87*, 363–380. (h) Sleight, A. W. In *Advanced Materials in Catalysis*; Burton, J. J., Garten, R. L., Eds.; Academic Press: New York, 1977; pp 181–208.
- (13) For early-transition-metal oxo species that display similar reactivity, see: (a) Carney, M. J.; Walsh, P. J.; Hollander, F. J.; Bergman, R. G. *J. Am. Chem. Soc.* **1989**, *111*, 8751–8753. (b) Parkin, G.; Bercaw, J. E. *J. Am. Chem. Soc.* **1989**, *111*, 391–393. (c) Herrmann, W. A.; Herdtweck, E.; Floel, M.; Kulpe, J.; Kusthardt, U.; Okuda, J. *Polyhedron* **1987**, *6*, 1165–1182.
- (14) Holm, R. H. *Chem. Rev.* **1987**, *87*, 1401–1449.

* Alfred P. Sloan Foundation Fellow (1987–1989).

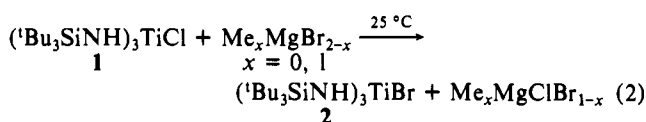
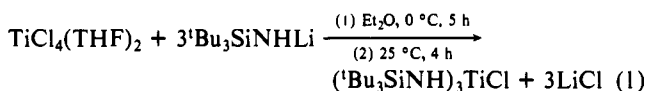
Table I. ^1H and ^{13}C NMR Data for $(^1\text{Bu}_3\text{SiNH})\text{Ti}$ and $^1\text{Bu}_3\text{SiN}=\text{Ti}$ Derivatives in Benzene- d_6

compound	^1H (δ , mult, J (Hz)) ^a				$^{13}\text{C}\{^1\text{H}\}$ (δ) ^b		
	$^1\text{Bu}_3\text{Si}(\text{NH},\text{N})^c$	HN	OR ₂	other	$^1\text{Bu}_3\text{Si}(\text{NH},\text{N})^d$	OR ₂	other
$(^1\text{Bu}_3\text{SiNH})_3\text{TiCl}$ (1)	1.28	8.32			31.17, 23.79		
$(^1\text{Bu}_3\text{SiNH})_3\text{TiBr}$ (2)	1.29	8.49			31.17, 23.76		
$(^1\text{Bu}_3\text{SiNH})_4\text{Ti}$ (12)	1.32	6.18			31.61, 23.75		
$(^1\text{Bu}_3\text{SiNH})_2(\text{Et}_2\text{O})\text{Ti}=\text{NSi}^i\text{Bu}_3$ (4)	1.32	5.50	0.87, t, 6.9		31.31, 23.36	12.89	
	1.40		4.13, q, 6.9		31.70, 24.24	69.85	
$(^1\text{Bu}_3\text{SiNH})_2(\text{THF})\text{Ti}=\text{NSi}^i\text{Bu}_3$ (13)	1.33	5.48	1.23, m		31.30, 23.31	25.19	
	1.41		1.33, m		31.70, 24.21	77.27	
$(^1\text{Bu}_3\text{SiNH})(\text{THF})\text{ClTi}=\text{NSi}^i\text{Bu}_3$ (9)	1.23	9.40	1.13, m		30.80, 24.14	25.14	
	1.38		3.93, m		31.09, 23.13	75.63	
$(^1\text{Bu}_3\text{SiNH})(\text{THF})\text{BrTi}=\text{NSi}^i\text{Bu}_3$ (11)	1.23	9.55	1.17, m		30.77, 23.15	25.10	
	1.38		4.01, m		31.07, 24.17	75.95	
$(^1\text{Bu}_3\text{SiNH})(\text{THF})\text{MeTi}=\text{NSi}^i\text{Bu}_3$ (15)	1.25	7.35	1.08, m	0.87 (Me)	30.81, 23.20	24.86	31.30 (Me)
	1.43		3.70, m		31.25, 24.23	73.67	
$(^1\text{Bu}_3\text{SiNH})(\text{THF})^i\text{BuTi}=\text{NSi}^i\text{Bu}_3$ (16)	1.29	6.11	1.10, m	1.59 (^iBu)	31.16, 23.38	25.01	32.45 (Me_3)
	1.42		3.97, m		31.58, 24.23	75.81	59.21 (TiC)
$[(^1\text{Bu}_3\text{SiNH})\text{Ti}]_2(\mu\text{-NSi}^i\text{Bu}_3)_2$ (17)	1.17	7.58			31.67, 24.46		
	1.25				31.31, 23.42		

^a Referenced to $\text{C}_6\text{D}_5\text{H}$ at δ 7.15 or TMS at δ 0.00. ^b Referenced to $\text{C}_6\text{D}_5\text{H}$ at δ 128.00. ^c The first value corresponds to the amide, the second to the imide. ^d The first line refers to the Me and tertiary carbons of the amide, the second to the imide. These assignments are tentative.

Results and Discussion

$(^1\text{Bu}_3\text{SiNH})_3\text{TiX}$ Derivatives. The slow (4–5 h) addition of $\text{TiCl}_4(\text{THF})_2$ to an ethereal solution containing 3 equiv of $^1\text{Bu}_3\text{SiNHLi}$,¹⁰ prepared from $^1\text{BuLi}$ and $^1\text{Bu}_3\text{SiNH}_2$,²¹ afforded colorless $(^1\text{Bu}_3\text{SiNH})_3\text{TiCl}$ (1; eq 1) in 82% yield after crystal-



lization from pentane. ^1H and $^{13}\text{C}\{^1\text{H}\}$ NMR data for all new compounds are listed in Table I. In contrast to the corresponding zirconium complex,^{10,11} methylation of chloride 1 was unsuccessful. Treatment of 1 with 1.0 equiv of MeMgBr in Et_2O yielded the bromide derivative, $(^1\text{Bu}_3\text{SiNH})_3\text{TiBr}$ (2), which could also be prepared via metathesis with excess MgBr_2 in THF (eq 2). Halogen exchange is likely to proceed via a dihalo-bridged intermediate, $(^1\text{Bu}_3\text{SiNH})_3\text{Ti}(\mu\text{-Cl})(\mu\text{-Br})\text{MgX}$ ($X = \text{Me, Br}$), that may constrain the approach of a MgMe group to the Ti center. Milder alkylating agents such as Me_2Zn and Me_3Al were ineffective under similar conditions.

Upon addition of a stoichiometric amount of MeLi to the chloride 1 in Et_2O , methane was produced as a consequence of

(15) (a) Buchwald, S. L.; Nielsen, R. B. *J. Am. Chem. Soc.* **1988**, *110*, 3171–3175. (b) Mayer, J. M.; Curtis, C. J.; Bercaw, J. E. *J. Am. Chem. Soc.* **1983**, *105*, 2651–2660. (c) Schock, L. E.; Brock, C. P.; Marks, T. J. *Organometallics* **1987**, *6*, 232–241. (d) McDade, C.; Green, J. C.; Bercaw, J. E. *Organometallics* **1982**, *1*, 1629–1634.

(16) For systems that undergo similar abstractions, see: (a) Nugent, W. A.; Ovenall, D. W.; Holmes, S. J. *Organometallics* **1983**, *2*, 161–162. (b) Nugent, W. A.; Zubyk, R. M. *Inorg. Chem.* **1986**, *25*, 4604–4606. (c) Takahashi, Y.; Onoyama, N.; Ishikawa, Y.; Motojima, S.; Sugiyama, K. *Chem. Lett.* **1978**, 525–528.

(17) Walsh, P. J.; Hollander, F. J.; Bergman, R. G. *J. Am. Chem. Soc.* **1988**, *110*, 8729–8731.

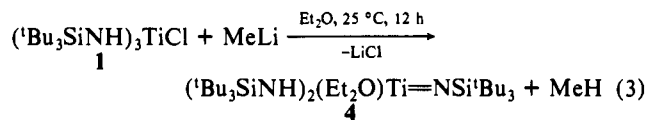
(18) (a) Nugent, W. A.; Mayer, J. M. *Metal-Ligand Multiple Bonds*; Wiley-Interscience: New York, 1988. (b) Chisholm, M. H.; Rothwell, I. P. In *Comprehensive Coordination Chemistry*; Pergamon Press: New York, 1987; Vol. 2, Chapter 13.4. (c) Nugent, W. A.; Haymore, B. L. *Coord. Chem. Rev.* **1980**, *31*, 123–175. (d) Harlan, E. W.; Holm, R. H. *J. Am. Chem. Soc.* **1990**, *112*, 186–193.

(19) (a) Hill, J. E.; Profflet, R. D.; Fanwick, P. E.; Rothwell, I. P. *Angew. Chem.* **1990**, *102*, 713–715. See also: (b) Hill, J. E.; Fanwick, P. E.; Rothwell, I. P. *Inorg. Chem.* **1989**, *28*, 3602–3606.

(20) Roessky, H. W.; Voelker, H.; Witt, M.; Noltemeyer, M. *Angew. Chem.* **1990**, *102*, 712–713.

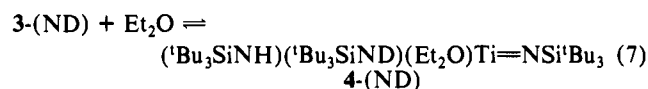
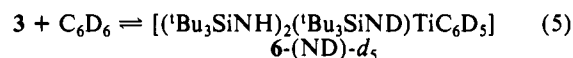
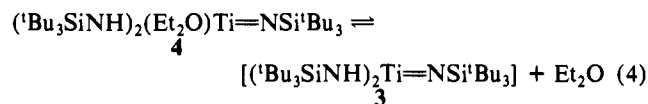
(21) Nowakowski, P. M.; Sommer, L. H. *J. Organomet. Chem.* **1979**, *178*, 95–103.

dehydrohalogenation,²² and an etherate of $[(^1\text{Bu}_3\text{SiNH})_2\text{Ti}=\text{NSi}^i\text{Bu}_3]$ (3) formed in ~85% yield (^1H NMR). Crystallization from hexane provided the bis(amido) imido complex, $(^1\text{Bu}_3\text{SiNH})_2(\text{Et}_2\text{O})\text{Ti}=\text{NSi}^i\text{Bu}_3$ (4), in ~55% yield (eq 3),



typically contaminated with 5–10% of unidentified byproducts. The reaction can be viewed in two ways: (1) deprotonation of an amide,²² followed by Cl^- loss, leads to 3, which is trapped by Et_2O ; (2) alkylation generates the desired methyl complex, $(^1\text{Bu}_3\text{SiNH})_3\text{TiMe}$ (5), but the latter is unstable with respect to loss of methane and formation of 3, which is again scavenged by Et_2O . Labeling studies designed to distinguish these pathways failed due to interference from the impurities.

When benzene- d_6 solutions of $(^1\text{Bu}_3\text{SiNH})_2(\text{Et}_2\text{O})\text{Ti}=\text{NSi}^i\text{Bu}_3$ (4) are thermolyzed at 97°C for 2 h, complete deuteration of the amido protons is observed. A sequence of reactions initiated by the dissociation of Et_2O from 4 (eq 4) provides a logical



explanation for H/D exchange between the amides and solvent, based on previous zirconium chemistry.¹¹ Transient imido $[(^1\text{Bu}_3\text{SiNH})_2\text{Ti}=\text{NSi}^i\text{Bu}_3]$ (3) adds a C—D bond of benzene- d_6 across the $\text{Ti}=\text{N}$ linkage (eq 5) to generate $[(^1\text{Bu}_3\text{SiNH})_2(^1\text{Bu}_3\text{SiND})\text{TiC}_6\text{D}_5]$ (6-(ND)- d_5). Elimination of $\text{C}_6\text{D}_5\text{H}$ from the latter provides $[(^1\text{Bu}_3\text{SiNH})(^1\text{Bu}_3\text{SiND})\text{Ti}=\text{NSi}^i\text{Bu}_3]$ (3-(ND); eq 6), which recaptures Et_2O to form 4-(ND) (eq 7), thereby completing one deuteration cycle.

Any process that generates an imido group apparently renders the amides susceptible to H/D exchange with deuterated solvents,

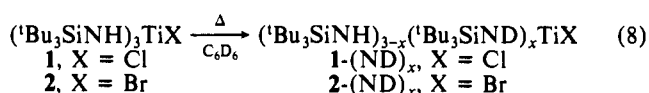
(22) For a related deprotonation of a NHSi^iBu_3 group, see: de With, J.; Horton, A. D.; Orpen, A. G. *Organometallics* **1990**, *9*, 2207–2209.

Table II. Selected Rate Constants^a for the Elimination of ^tBu₃SiNH₂ from (^tBu₃SiNH(D))₃TiX (X = Cl (1) (1-ND)₃), Br (2), ^tBu₃SiNH (12) in C₆D₆ with Added THF-*d*₈

X	[(^t Bu ₃ SiNH) ₃ TiX] (M)	[THF- <i>d</i> ₈] (M)	<i>k</i> (×10 ⁴ s ⁻¹) ^a	<i>T</i> (±0.3 °C)
Cl (1)	0.0294 (6)	0.444	0.146 (3)	60.0 ^b
	0.0294 (6)	0.444	0.44 (1)	71.7 ^b
	0.030 (3)	0.444	1.03 (1)	80.5 ^b
	0.030 (3)	0.222	0.967 (5)	80.5
	0.030 (3)	0.111	1.02 (1)	80.2
	0.030 (3)	5.55	1.40 (3)	81.0 ^c
	0.030 (3)	11.1	1.46 (3)	81.0 ^d
	0.083 (3)	0.444	1.1 (2)	81.7
	0.083 (3)	0.444	2.49 (2)	90.2 ^b
	0.030 (3)	0.444	1.9 (2)	90.4 ^e
	0.030 (3)	0.444	6.80 (7)	100.5 ^b
	0.030 (3)	0.444	16.5 (2)	110.4 ^b
	Cl (1-ND) ₃	0.030 (3)	0.444	0.32 (2)
Br (2)	0.014 (1)	0.444	0.97 (2)	81.4
^t Bu ₃ SiNH (12)	0.025 (1)	0.444	10.4 (3)	80.8

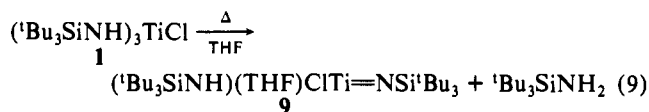
^a Determined from weighted, nonlinear, least-squares fitting of the differential form of the rate expression. ^b Values used in the Eyring plot (60.0–110.4 °C). From a weighted, nonlinear, least-squares fit of the data: $\Delta H^\ddagger = 23.3$ (8) kcal/mol, $\Delta S^\ddagger = -11$ (2) eu. ^c 1:1 THF-*d*₈ to C₆D₆. ^d Neat THF-*d*₈. ^e Tandem measurement.

provided a coordination site is available. Thermolysis of the tris(amido) halides, (^tBu₃SiNH)₃TiX (X = Cl (1), 17% deuteration (110 °C, 12 h); Br (2), >95% deuteration (110 °C, 12 h)) also resulted in deuteration of the amide positions, as eq 8 il-



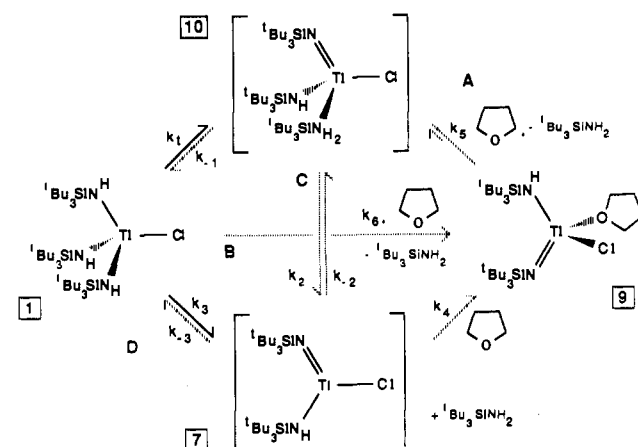
lustrates. Loss of either HX or ^tBu₃SiNH₂ would produce a Ti=N unit capable of mediating H/D exchange, although the former is less likely in view of the robust nature of these systems. A three-coordinate haloimido complex, (^tBu₃SiNH)XTi=NSi^tBu₃ (X = Cl (7), Br (8)), would be produced upon amine loss,¹⁷ and the subsequent addition/elimination of benzene-*d*₆ to the Ti=N linkage, followed by recapture of ^tBu₃SiNH₂, would constitute a deuteration cycle akin to eqs 4–7.²³

Evidence for the loss of amine was established by the trapping of chloroimido 7 during thermolysis of (^tBu₃SiNH)₃TiCl (1) in THF (eq 9). Adduct formation was observed and



(^tBu₃SiNH)(THF)CITi=NSi^tBu₃ (9) was isolated upon precipitation from pentane (83% yield). Bergman et al. have proposed a similar elimination of RNH₂ from Cp₂Zr(NHR)₂ to produce intermediate [Cp₂Zr=NR].¹⁷ This transient was also shown to activate arene C–H bonds and could be trapped by tetrahydrofuran. A potentially interesting analogy to alkane elimination from (^tBu₃SiNH)₃ZrR¹¹ presented itself; hence an investigation into the mechanism of amine loss from 1 was undertaken.

Mechanistic Investigation of (^tBu₃SiNH)(THF)CITi=NSi^tBu₃ (9) Formation. The extrusion of ^tBu₃SiNH₂ from (^tBu₃SiNH)₃TiCl (1) to form (^tBu₃SiNH)(THF)CITi=NSi^tBu₃ (9) was conveniently monitored in benzene-*d*₆ with variable amounts of THF added by following their respective amido protons with ¹H NMR spectroscopy. Selected rate constants (e.g., *k*_{obs} = 1.03 (1) × 10⁻⁴ s⁻¹ at 80.5 °C) for loss of amine (eq 9) are listed in Table II. No intermediates were directly observed, and the reaction is first order in [1]. Added ^tBu₃SiNH₂ did not inhibit the rate, and no dependence on [THF-*d*₈] was observed

Scheme I

(0.111–0.444 M), even though these low concentrations only represent 3.7–14.8 equiv of THF-*d*₈/equiv of 1. One may surmise that the step or steps utilizing THF are not only post rate determining, but extremely swift, since the THF-*d*₈ to 1 ratio was much lower than in typical pseudo-first-order conditions. In neat THF-*d*₈ or a 1:1 mixture of C₆D₆/THF-*d*₈, a slight increase in rate was observed (THF-*d*₈; *k*_{obs} = 1.46 (3) × 10⁻⁴ s⁻¹, 81.0 °C); hence, the effects of the medium, presumably outer sphere, are rather minor considering the dramatic change in dielectric.

Rate constants acquired at six temperatures (60.0–110.4 °C) were used to generate activation parameters from an Eyring plot. The values obtained ($\Delta H^\ddagger = 23.3$ (8) kcal/mol, $\Delta S^\ddagger = -11$ (2) eu) are consistent with a substantial amount of bond breaking in a transition state that is somewhat ordered. Methane elimination from (^tBu₃SiNH)₃ZrMe was described by comparable activation parameters ($\Delta H^\ddagger = 25.9$ (4) kcal/mol, $\Delta S^\ddagger = -7$ (1) eu),¹¹ perhaps indicative of mechanistic similarities.

Scheme I illustrates four plausible mechanisms for the conversion of (^tBu₃SiNH)₃TiCl (1) to (^tBu₃SiNH)(THF)CITi=NSi^tBu₃ (9) and ^tBu₃SiNH₂. In A (1 → 10 → 9), proton transfer (*k*₁) produces an imido amido amine intermediate, [(^tBu₃SiNH)(^tBu₃SiNH₂)CITi=NSi^tBu₃] (10), that undergoes associative substitution (*k*₅) of bound ^tBu₃SiNH₂ by THF. The resulting rate expression, $-d[1]/dt = k_1 k_5 [1] [\text{THF}] / (k_{-1} + k_5 [\text{THF}])$, predicts the reaction to be first order in THF if proton transfer is fast and reversible, a reasonable supposition. In corroboration, Nugent et al. reported rapid, reversible proton transfers between imido and amine ligands bound to tungsten(VI).^{24,25}

A solvent-assisted 1,2-elimination of amine from 1 represents another possibility (B: 1 → 9), one depicted as a continuous pathway with no intermediates (i.e., $-d[1]/dt = k_6 [1] [\text{THF}]$). However, pathway B or kinetically indistinguishable mechanisms requiring five-coordinate intermediates can be eliminated with confidence, since a [THF] dependence was not found.

Pathway C (1 → 10 → 7 → 9) again invokes proton transfer (*k*₁), but this is followed by amine dissociation (*k*₂) and trapping of chloro imido 7 (*k*₄) by THF. In this dissociative case, the rate ($-d[1]/dt = k_1 k_2 k_4 [1] [\text{THF}] / (k_{-1} k_2 [\text{}^t\text{Bu}_3\text{SiNH}_2] + k_{-1} k_4 [\text{THF}] + k_2 k_4 [\text{THF}])$) will be first order in [THF] only if proton transfer is reversible and amine effectively competes (*k*₂) with THF for capture of 7. If proton transfer is rate determining in either A or C, or amine dissociation (*k*₂) in C, no order in [THF] will be observed.

Mechanism D (1 → 7 → 9) is based on the abstraction of an amide proton by a neighboring amide group (*k*₃), a process analogous to that proposed for the 1,2-elimination of RH from

(24) (a) Chan, D. M.-T.; Fultz, W. C.; Nugent, W. A.; Roe, D. C.; Tulip, T. H. *J. Am. Chem. Soc.* **1985**, *107*, 251–253. See also: (b) Jones, C. M.; Lerchen, M. E.; Church, C. J.; Schomber, B. M.; Doherty, N. M. *Inorg. Chem.* **1990**, *29*, 1679–1682.

(25) For similar proton transfers, see: (a) Edwards, D. S.; Schrock, R. R. *J. Am. Chem. Soc.* **1982**, *104*, 6806–6808. (b) Rocklage, S. M.; Schrock, R. R.; Churchill, M. R.; Wasserman, H. J. *Organometallics* **1982**, *1*, 1332–1338.

(23) It is possible that amine loss from 4 is responsible for deuteration of the amido hydrogens, instead of eqs 4–7. However, the conditions required for deuteration are much milder than for 1, and efforts directed toward amine elimination to form a bis(imido) derivative have been unsuccessful. Cummins, C. C.; Wolczanski, P. T., unpublished results.

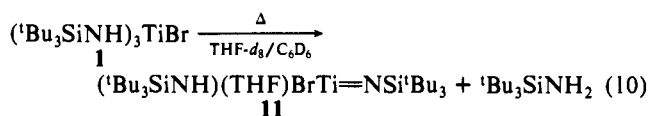
(¹Bu₃SiNH)₃ZrR. If this is reversible, the reaction will be first order in [THF] and inhibited by added amine (*k*₋₃), since the transient chloro imido **7** scavenges THF to produce **9** (e.g., $-d[1]/dt = k_3 k_4 [1][\text{THF}] / (k_{-3} [{}^1\text{Bu}_3\text{SiNH}_2] + k_4 [\text{THF}])$). If the abstraction is irreversible, the rate will be independent of [THF].

Given the [THF-*d*₈] independence, *k*_{obs} may refer to *k*₁, proton transfer (either A or C), *k*₃, abstraction of an amido hydrogen by a leaving amide group (D), or (*k*₁/*k*₋₁)*k*₂, a preequilibrium proton transfer followed by rate-determining amine loss (C). The lack of inhibition by added ¹Bu₃SiNH₂ unfortunately fails to rule out any remaining scheme. When the rate of disappearance of **1** vs (¹Bu₃SiND)₃TiCl (**1**-(ND)₃) was compared, a substantial kinetic isotope effect (*k*(NH)₃/*k*(ND)₃ at 90.4 °C) of 5.9 (**6**) was observed, effectively ruling out C, since an isotope effect of this magnitude cannot be attributed to a preequilibrium.²⁶ Kinetic isotope effects in this range have been observed previously for numerous abstraction processes,^{15,16} including the elimination of CH₄ vs CH₃D from (¹Bu₃SiNH/D)₃ZrMe, where *k*(NH)₃/*k*(ND)₃ = 7.3 (**4**) at 97 °C.¹¹

It is interesting to note that no deuteration of the amido positions of **1** or **9** was detected during the course of these studies, indicating that THF-*d*₈ effectively competes with C₆D₆ for either intermediate (**7** or **10**). Assuming that 10% deuteration of the NH groups in **1** or **9** could be detected, at [THF-*d*₈] = 0.111 M the scavenging of either **7** or **10** by THF-*d*₈ is roughly ≥ 10³ faster than trapping by C₆D₆.²⁷

Attempts to differentiate between associative pathway A and C or D by carrying out the reaction in the opposite direction failed, although the microscopic reverse was observed. Extensive thermolysis (91 °C) of **9** in the presence of deuterated amine, ¹Bu₃SiND₂, caused the deuteration of its amido position, and the rate (~10⁻³ M⁻¹ s⁻¹) was dependent upon [¹Bu₃SiND₂] while inhibited by THF.²⁸ Unfortunately, the conditions promoted undesirable side reactions; hence, these efforts were abandoned.

Similar geometries of (¹Bu₃SiNH)₃TiCl (**1**) and hypothetical [(¹Bu₃SiNH)(¹Bu₃SiNH₂)ClTi=NSi¹Bu₃] (**10**) suggest that an amide to amide proton transfer (*k*₁) would be reversible (*k*₋₁).²⁴ Furthermore, the characteristics (i.e., activation parameters, *k*(NH)₃/*k*(ND)₃, etc.) of amine loss from **1** convincingly parallel the methane extrusion from (¹Bu₃SiNH/D)₃ZrMe, a reaction best described as an abstraction. In an NMR tube reaction, thermolysis of (¹Bu₃SiNH)₃TiBr (**2**) under standard conditions provided (¹Bu₃SiNH)(THF)BrTi=NSi¹Bu₃ (**11**; eq 10), but the rate (*k*_{obs}



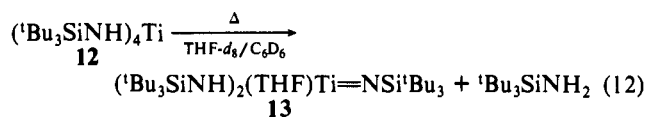
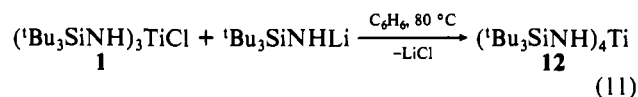
= 9.7 (**4**) × 10⁻⁵ s⁻¹ at 81.4 °C) was within error of the chloride **1** thermolysis. While the experiment suggests that the Br⁻ substituent has no effect, the interpretation of this result may be more subtle. Chloride is generally considered to form stronger early-transition-metal π-bonds than Br⁻; thus three-coordinate intermediate **7** should be more stabilized than its bromide counterpart. Assuming the transition state resembles **7**, this stabilization should be reflected in the relative disappearance rates of **1** vs **2**; however, the different halides may comparably effect the relative ground-state energies of **1** and **2**; hence the similar rates may simply indicate that the substitution of Br⁻ for Cl⁻ effects both ground and transition states equally.

(26) Carpenter, B. K. *Determination of Organic Reaction Mechanisms*; Wiley-Interscience: New York, 1984.

(27) At [THF-*d*₈] = 0.111 M, [C₆D₆] ~ 11.2 M. Neglecting kinetic isotope effects present in the deuteration cycle and given the stated observation limit of 10%, the trapping ratio *k*_{THF}[THF-*d*₈]/*k*_{benzene}[C₆D₆] = 10, hence *k*_{THF}/*k*_{benzene} ≥ 10³.

(28) At [¹Bu₃SiND₂] = 0.345 M, the pseudo-first-order rate constant *k* = 3.0 × 10⁻⁴ (91 °C); at [¹Bu₃SiND₂] = 0.691 M, *k* = 7.0 × 10⁻⁴ (91 °C). Note that in principle, both A and C would exhibit regimes where deuteration rate is independent of [¹Bu₃SiND₂], provided concentrations of the latter are high. Alternatively stated, the intercepts of 1/*k*_{obs} vs 1/[¹Bu₃SiND₂] plots for mechanisms A and C would be independent of [¹Bu₃SiND₂], whereas the intercept for A would be dependent on [¹Bu₃SiND₂].

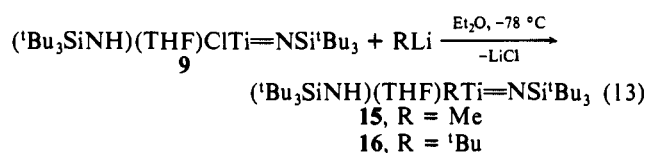
Differentiation on a steric basis seemed plausible, because a rate-determining proton transfer (*k*₁) generates four-coordinate **10**, while abstraction (*k*₃) produces three-coordinate **7**. Treatment of (¹Bu₃SiNH)₃TiCl (**1**) with ¹Bu₃SiNHLi at 80 °C in benzene afforded (¹Bu₃SiNH)₄Ti (**12**) in 59% yield (eq 11). Tetraamido



12 was smoothly converted to (¹Bu₃SiNH)₂(THF)Ti=NSi¹Bu₃ (**13**) in C₆D₆ with 18 equiv of THF-*d*₈ present (eq 12). Its rate of disappearance was measured to be ~10 times faster (*k*_{obs} = 1.04 (**3**) × 10⁻³ s⁻¹ at 80.8 °C) than **1** under similar conditions. Given the comparable geometries of (¹Bu₃SiNH)₄Ti (**12**) and the hypothetical proton-transfer intermediate [(¹Bu₃SiNH)₂(¹Bu₃SiNH₂)Ti=NSi¹Bu₃] (**14**), a significant change in rate would not be expected on the basis of steric considerations. However, an abstraction pathway leading to three-coordinate [(¹Bu₃SiNH)₂Ti=NSi¹Bu₃] (**3**) should show a marked increase in rate upon substitution of Cl⁻ by ¹Bu₃SiNH⁻. This argument ignores electronic effects that are admittedly difficult to assess, especially in view of the above Cl⁻ vs Br⁻ results.

In view of the tetraamide thermolysis rate, the somewhat dubious nature of an irreversible proton transfer in this system, and the aforementioned parallels to methane loss from (¹Bu₃SiNH)₃ZrMe,¹¹ abstraction pathway D is the most likely mechanism for the loss of amine from **1** to form **9**. The mechanistic alternatives in this system represent a continuum with two extremes. One is proton transfer, in which an amide NH bond is broken and an amine one created prior to a distinctly separate TiN bond-breaking event. The opposite extreme requires the amide TiN bond to be broken prior to abstraction of an adjacent amido hydrogen. The abstraction process probed by the kinetics experiments is probably best viewed as intermediate between these extremes; the amido hydrogen is abstracted with concomitant TiN bond breaking akin to a concerted 1,2-elimination.

Hydrogenation of (¹Bu₃SiNH)(L)RTi=NSi¹Bu₃. Alkylation of (¹Bu₃SiNH)(THF)ClTi=NSi¹Bu₃ (**9**) was accomplished via stoichiometric addition of MeLi or ¹BuLi in Et₂O at -78 °C (eq 13) to form off-white (¹Bu₃SiNH)(THF)MeTi=NSi¹Bu₃ (**15**;



55%) and yellow (¹Bu₃SiNH)(THF)¹BuTi=NSi¹Bu₃ (**16**; 76%). Amido imido methyl **15** degraded slowly in the reaction medium, but was thermally stable after trituration and crystallization from hexane. The thermally unstable ¹Bu derivative **16** was precipitated from pentane and conveniently stored at -20 °C. Isolable early-transition-metal ¹Bu derivatives are rare entities, since rearrangements to isobutyl complexes via a β-elimination/insertion pathways are common. Unlike ¹Bu₄Cr,²⁹ which is apparently sterically constrained from undergoing β-elimination, **16** may be related to compounds³⁰⁻³³ that are stabilized elec-

(29) Kruse, W. *J. Organomet. Chem.* **1972**, *42*, C39-C42.

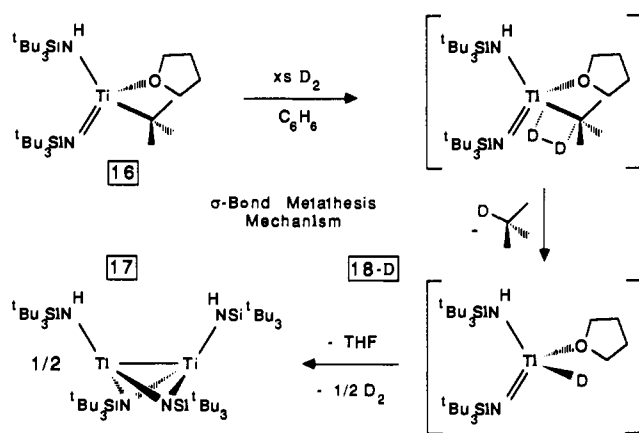
(30) (a) Buchwald, S. L.; Kreutzer, K. A.; Fisher, R. A. *J. Am. Chem. Soc.* **1990**, *112*, 4600-4601. (b) Buchwald, S. L.; Lum, R. T.; Fisher, R. A.; Davis, W. M. *J. Am. Chem. Soc.* **1989**, *111*, 9113-9114.

(31) Chisholm, M. H.; Tan, L.-S.; Huffman, J. C. *J. Am. Chem. Soc.* **1982**, *104*, 4879-4884.

(32) (a) Burger, H.; Neese, H. *J. Organomet. Chem.* **1969**, *20*, 129-139. (b) Burger, H.; Neese, H. *J. Organomet. Chem.* **1970**, *21*, 381-388.

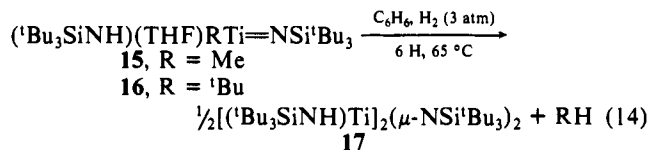
(33) Chisholm, M. H.; Folting, K.; Haitko, D. A.; Huffman, J. C. *J. Am. Chem. Soc.* **1981**, *103*, 4046-4053.

Scheme II



tronically, such as $\text{Cp}_2\text{MX}(\text{tBu})^{30}$ and $(\text{Me}_2\text{N})_4\text{Ta}(\text{tBu})^{31}$. Chisholm³¹ has remarked that strong π -donor ligands stabilize alkyls by utilizing and therefore raising the energy of metal-based orbitals that would typically participate in β -elimination reactions.

Exposure of the alkyl complexes, $(\text{tBu}_3\text{SiNH})(\text{THF})\text{RTi}=\text{NSi}^i\text{Bu}_3$ ($\text{R} = \text{Me}$ (**15**), tBu (**16**)), to dihydrogen (3 atm) in benzene for 3 h at 65 °C led to the formation of $[(\text{tBu}_3\text{SiNH})\text{Ti}]_2(\mu\text{-NSi}^i\text{Bu}_3)_2$ (**17**) and concomitant methane or isobutane, respectively (eq 14). Amido imido dimer **17** was isolated from



Et_2O in 61% yield when **15** was the precursor, while ^1H NMR experiments indicated a $\sim 97\%$ conversion. Verification of a metal-metal single bond between the d^1 Ti(III) centers was achieved via X-ray crystallography (vide infra).

Scheme II displays the σ -bond metathesis³⁴ mechanism thought to be responsible for the formation of $[(\text{tBu}_3\text{SiNH})\text{Ti}]_2(\mu\text{-NSi}^i\text{Bu}_3)_2$ (**17**). Evidence for the process rests with the following observations. Toepler pump measurements indicated that 0.48 equiv of H_2 /equiv of **16** were consumed in the reaction. The conversion of **16** and $1/2 \text{D}_2$ to **17** was monitored by ^1H NMR (C_6D_6) and only DCMe₃ ($>95\%$ by ^1H NMR) was produced. Only minor deuterium incorporation ($\sim 13\%$) into the amido position of $(\text{tBu}_3\text{SiNH})(\text{THF})\text{tBuTi}=\text{NSi}^i\text{Bu}_3$ (**16**) was seen near the conclusion of the reaction. Reversible addition of D_2 across the imido bond of **16** would have deuterated its tBu_3SiNH . An irreversible addition of D_2 to form $[(\text{tBu}_3\text{SiNH})(\text{tBu}_3\text{SiND})(\text{THF})\text{TiD}(\text{tBu})]$ can also be ruled out; careful examination of the dimer **17** revealed that no deuterium ($<3\%$) was incorporated in its amido positions throughout the course of the reaction. If $[(\text{tBu}_3\text{SiNH})(\text{tBu}_3\text{SiND})(\text{THF})\text{TiD}(\text{tBu})]$ were an intermediate, reductive elimination to give DCMe_3 would have generated $[(\text{tBu}_3\text{SiNH})(\text{tBu}_3\text{SiND})(\text{THF})\text{Ti}]$ as a transient. Dimerization and rearrangement of this species would have resulted in immediate deuterium incorporation in the amido site of **17**. Furthermore, a 1,2-elimination of isobutane from $[(\text{tBu}_3\text{SiNH})(\text{tBu}_3\text{SiND})(\text{THF})\text{TiD}(\text{tBu})]$ would have produced unlabeled HCMe_3 .

The product-forming step of the reaction can be viewed as a dimerization of transient hydride $[(\text{tBu}_3\text{SiNH})(\text{THF})\text{DTi}=\text{NSi}^i\text{Bu}_3]$ (**18-D**) with concomitant D_2 loss, or a dinuclear reductive elimination of DCMe_3 from **18-D** and $(\text{tBu}_3\text{SiNH})(\text{THF})\text{tBuTi}=\text{NSi}^i\text{Bu}_3$ (**16**). In principle, the two mechanisms may be distinguished by using a 1:1 mixture of H_2 and D_2 . If the hydride dimerization pathway were operative, HD would immediately be generated from the reaction of **18** and **18-D**. Unfortunately, **17** was found to catalyze the scrambling of H_2 and D_2 (0.75 atm total, 100 equiv/**17**), thereby making this study experimentally untenable. After 1.5 h at 60 °C, 17 equiv of HD/**17** was produced. These observations suggest that the transient hydride **18** may be formed from **17**, thereby supporting the dinuclear H_2 -elimination segment of Scheme II from the standpoint of microscopic reversibility.

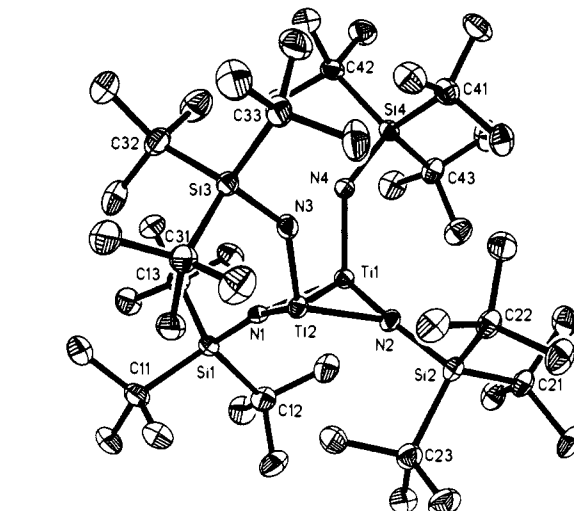
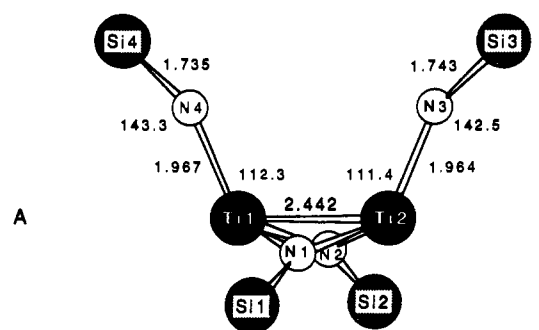


Figure 1. Molecular view of $[(\text{tBu}_3\text{SiNH})\text{Ti}]_2(\mu\text{-NSi}^i\text{Bu}_3)_2$ (**17**).



Ti deviations from 3 N plane: 0.58 and 0.60 Å

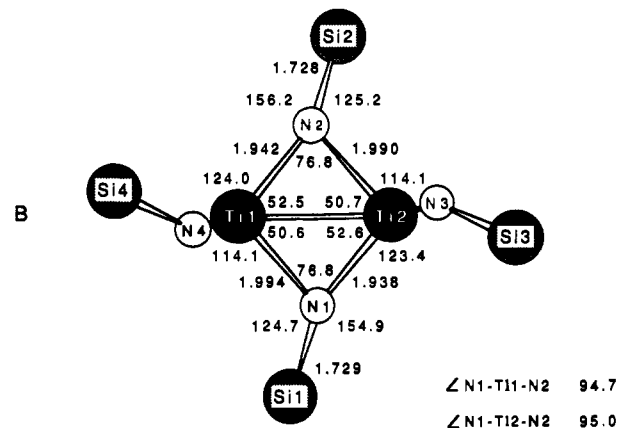


Figure 2. Skeletal views of $[(\text{tBu}_3\text{SiNH})\text{Ti}]_2(\mu\text{-NSi}^i\text{Bu}_3)_2$ (**17**). Bond distances are in angstroms and bond angles are in degrees.

NSi^iBu_3 (**18-D**) with concomitant D_2 loss, or a dinuclear reductive elimination of DCMe_3 from **18-D** and $(\text{tBu}_3\text{SiNH})(\text{THF})\text{tBuTi}=\text{NSi}^i\text{Bu}_3$ (**16**). In principle, the two mechanisms may be distinguished by using a 1:1 mixture of H_2 and D_2 . If the hydride dimerization pathway were operative, HD would immediately be generated from the reaction of **18** and **18-D**. Unfortunately, **17** was found to catalyze the scrambling of H_2 and D_2 (0.75 atm total, 100 equiv/**17**), thereby making this study experimentally untenable. After 1.5 h at 60 °C, 17 equiv of HD/**17** was produced. These observations suggest that the transient hydride **18** may be formed from **17**, thereby supporting the dinuclear H_2 -elimination segment of Scheme II from the standpoint of microscopic reversibility.

X-ray Crystal Structure of $[(\text{tBu}_3\text{SiNH})\text{Ti}]_2(\mu\text{-NSi}^i\text{Bu}_3)_2 \cdot \text{C}_6\text{H}_6$ (17**· C_6H_6).** A single-crystal X-ray structural determination

(34) (a) Thompson, M. E.; Baxter, S. M.; Bulls, A. R.; Burger, B. J.; Nolan, M. C.; Santarsiero, B. D.; Schaefer, W. P.; Bercaw, J. E. *J. Am. Chem. Soc.* **1987**, *109*, 203–219. (b) Gell, K. I.; Posin, B.; Schwartz, J.; Williams, G. M. *J. Am. Chem. Soc.* **1982**, *104*, 1846–1855. (c) Watson, P. L. *J. Am. Chem. Soc.* **1983**, *105*, 6491–6493. (d) Watson, P. L.; Parshall, G. W. *Acc. Chem. Res.* **1985**, *18*, 51–56. (e) Fendrick, C. M.; Marks, T. J. *J. Am. Chem. Soc.* **1986**, *108*, 425–437. (f) Jeske, G.; Lauke, H.; Mauermann, H.; Schumann, H.; Marks, T. J. *J. Am. Chem. Soc.* **1985**, *107*, 8111–8118. (g) Halpern, J. *Inorg. Chem. Acta* **1985**, *100*, 41–48.

Table III. Selected Interatomic Distances and Angles for $[(^t\text{Bu}_3\text{SiNH})\text{Ti}]_2(\mu\text{-NSi}^t\text{Bu}_3)_2\text{C}_6\text{H}_6$ (**17**)

Distances (Å)					
Ti1–Ti2	2.442 (1)	Ti1–N1	1.994 (4)	Ti1–N2	1.942 (4)
Ti1–N4	1.967 (4)	Ti2–N1	1.938 (3)	Ti2–N2	1.990 (4)
Ti2–N3	1.964 (4)	N1–Si1	1.729 (3)	N2–Si2	1.728 (4)
N3–Si3	1.743 (4)	N4–Si4	1.735 (4)	Si _{imido} –C	1.950 (7) _{av}
Si _{amido} –C	1.942 (6) _{av}	C–C	1.547 (7) _{av}		

Angles (deg)					
Ti2–Ti1–N1	50.6 (1)	Ti1–N2–Ti2	76.8 (1)		
Ti1–Ti2–N1	52.6 (1)	Ti1–N4–Si4	143.3 (2)		
N1–Ti1–N2	94.7 (1)	Ti2–N3–Si3	142.5 (2)		
N1–Ti2–N2	95.0 (2)	Si _{imido} –C–C	111.7 (24) _{av}		
Ti1–N1–Ti2	76.8 (1)	C–C–C	107.1 (11) _{av}		
Ti1–N2–Si2	156.2 (2)	Ti2–Ti1–N4	112.3 (1)		
Ti2–N2–Si2	125.2 (2)	Ti1–Ti2–N3	111.8 (1)		
N _{amido} –Si–C	107.5 (19) _{av}	N2–Ti1–N4	124.0 (1)		
C–Si–C	111.0 (6) _{av}	N2–Ti2–N3	114.1 (1)		
Ti2–Ti1–N2	52.5 (1)	Ti1–N1–Si1	124.7 (2)		
Ti1–Ti2–N2	50.7 (1)	Ti2–N1–Si1	154.9 (2)		
N1–Ti1–N4	114.1 (2)	N _{imido} –Si–C	108.2 (33) _{av}		
N1–Ti2–N3	123.4 (2)	Si _{amido} –C–C	111.7 (20) _{av}		

(monoclinic, $P2_1/n$) confirmed the dimeric nature of $[(^t\text{Bu}_3\text{SiNH})\text{Ti}]_2(\mu\text{-NSi}^t\text{Bu}_3)_2$ (**17**), as illustrated by the molecular view in Figure 1. Although crystallographically distinct, the independent halves of the complex are essentially equivalent. The skeletal views depicted in Figure 2 reveal the C_2 molecular symmetry of the dimer, clearly manifested by the asymmetric bonding of the bridging imido units.³⁵ Each titanium resides at the apex of a trigonal pyramid whose basal plane comprises nitrogens from an amide and two $\mu\text{-NSi}^t\text{Bu}_3$ bridges (N1, N2). Surprisingly, the two titanium atoms (Ti1, Ti2) are 0.58 and 0.60 Å exo to the N1–N2–N4 and N1–N2–N3 basal planes, respectively, and appear to be oriented toward empty space. Furthermore, none of the C–H bonds of the ^tBu groups are positioned to form agostic interactions with the metals.³⁶ Despite their locations outside the butterfly arrangement of the four nitrogens, the titaniums are only 2.442 (1) Å apart (Table III). Previously reported dititanium distances are greater than 2.7 Å,^{18,35,37–39} and the majority of these constitute Ti(IV)···Ti(IV) interactions where no metal–metal bond exists.^{35,37,38} Pasynskii recently reported the structure of

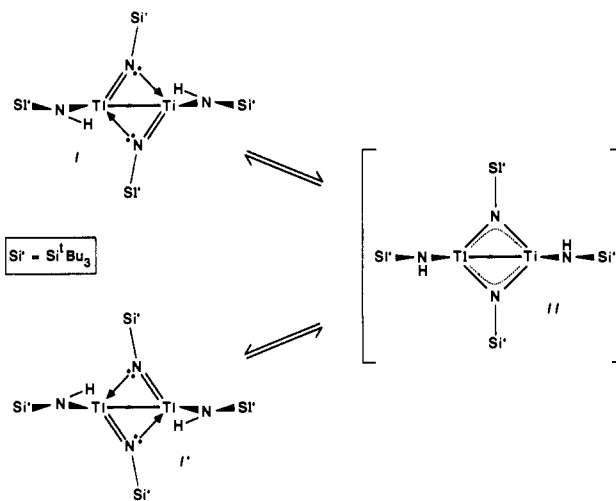
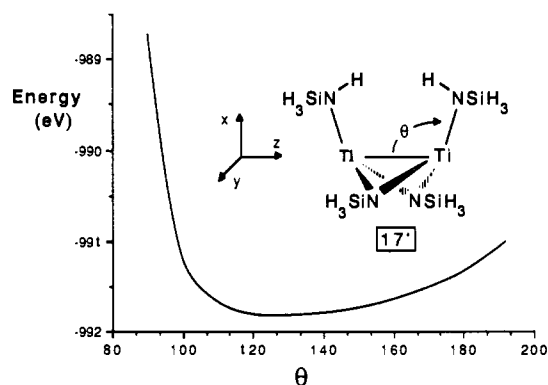
(35) For structural and theoretical treatments of asymmetric (e.g., $[\text{Me}_2(^t\text{BuN})\text{W}]_2(\mu\text{-N}^t\text{Bu}_2)$) vs symmetric (e.g., $[(\text{Me}_2\text{N})_2\text{Ti}]_2(\mu\text{-N}^t\text{Bu}_2)$) imido bridges, see: Thorn, D. L.; Nugent, W. A.; Harlow, R. L. *J. Am. Chem. Soc.* **1981**, *103*, 357–363, and references therein. In view of the treatment by Thorn et al., it is interesting to view the nonplanar C_2 geometry of $[(^t\text{Bu}_3\text{SiNH})\text{Ti}]_2(\mu\text{-NSi}^t\text{Bu}_3)_2$ (**17**) as a severe distortion from planarity that occurs solely to maximize π -bonding, regardless of the Ti–Ti bond.

(36) (a) Brookhart, M.; Green, M. L. H.; Wung, L. H. *Prog. Inorg. Chem.* **1988**, *36*, 1–124. (b) Brookhart, M.; Green, M. L. H. *J. Organomet. Chem.* **1983**, *250*, 395–408.

(37) For complexes containing reduced Ti centers less than ~ 3.0 Å apart, see: (a) Darkwa, J.; Lockemeyer, J. R.; Boyd, P. D. W.; Rauchfuss, T. B.; Rheingold, A. L. *J. Am. Chem. Soc.* **1988**, *110*, 141–149. (b) Bottomley, F.; Egharevba, G. O.; White, P. S. *J. Am. Chem. Soc.* **1985**, *107*, 4353–4354. (c) Huffman, J. C.; Stone, J. G.; Krussell, W. C.; Caulton, K. G. *J. Am. Chem. Soc.* **1977**, *99*, 5829–5830. (d) Roth, A.; Floriani, C.; Chiesi-Villa, A.; Guastini, C. *J. Am. Chem. Soc.* **1986**, *108*, 6823–6825. (e) Guggenberger, L. J.; Tebbe, F. N. *J. Am. Chem. Soc.* **1973**, *95*, 7871–7872. (f) Guggenberger, L. J.; Tebbe, F. N. *J. Am. Chem. Soc.* **1976**, *98*, 4137–4143. (g) Veldman, E. E.; Van der Wal, H. R.; Veenstra, S. J.; de Liefde Meijer, H. J. *J. Organomet. Chem.* **1980**, *197*, 59–65. (h) Hill, J. E.; Nash, J. M.; Fanwick, P. E.; Rothwell, I. P. *Polyhedron* **1990**, *9*, 617–619.

(38) For μ -imido complexes, see: (a) Gambarotta, S.; Floriani, C.; Chiesi-Villa, A.; Guastini, C. *J. Am. Chem. Soc.* **1983**, *105*, 7295–7301. (b) Vroegop, C. T.; Teuben, J. H.; van Bolhuis, F.; van der Linden, J. G. M. *J. Chem. Soc., Chem. Commun.* **1983**, 550–552. (c) Armor, J. N. *Inorg. Chem.* **1978**, *17*, 203–213. (d) Alcock, N. W.; Pierce-Butler, M.; Willey, G. R. *J. Chem. Soc., Dalton Trans.* **1976**, 707–713.

(39) For complexes containing Ti(IV) centers less than 3.0 Å apart, see: (a) Zank, G. A.; Jones, C. A.; Rauchfuss, T. B.; Rheingold, A. L. *Inorg. Chem.* **1986**, *25*, 1886–1891. (b) Borgias, B. A.; Cooper, S. R.; Koh, Y. B.; Raymond, K. N. *Inorg. Chem.* **1984**, *23*, 1009–1017. (c) Hughes, D. L.; Latham, I. A.; Leigh, G. J. *J. Chem. Soc., Dalton Trans.* **1986**, 393–398. (d) Schmidbaur, H.; Pichl, R.; Müller, G. *Angew. Chem., Int. Ed. Engl.* **1986**, *25*, 574–575. (e) Smith, G. D.; Caughlan, C. N.; Campbell, J. A. *Inorg. Chem.* **1972**, *11*, 2989–2993. (f) Bottomley, F.; Egharevba, G. O.; Lin, I. J. B.; White, P. S. *Organometallics* **1985**, *4*, 550–553.

**Figure 3.** Interconversion of two plausible resonance structures of $[(^t\text{Bu}_3\text{SiNH})\text{Ti}]_2(\mu\text{-NSi}^t\text{Bu}_3)_2$ (**17**).**Figure 4.** Energy (eV) of $[(\text{H}_3\text{SiNH})\text{Ti}]_2(\mu\text{-NSiH}_3)_2$ (**17'**), a model complex of $[(^t\text{Bu}_3\text{SiNH})\text{Ti}]_2(\mu\text{-NSi}^t\text{Bu}_3)_2$ (**17**), as a function of both Ti–Ti–N_{amide} angles, each defined by θ ($90^\circ \leq \theta \leq 190^\circ$).

$[\text{CpV}]_2(\mu\text{-NPh})(\mu\text{-N}_2\text{Ph}_2)$, a complex that contains a similarly short V–V bond (2.420 (6) Å) supported by bridging phenylimido units.⁴⁰

In general, the strength of the interaction between unsaturated monomers is determined by the electronic compensation gained through the formation of metal–metal and bridge bonds.^{3,4} The presumed linear, two-coordinate $(^t\text{Bu}_3\text{SiNH})\text{Ti}=\text{NSi}^t\text{Bu}_3$ is considered to possess at most 11 valence electrons. Although dimerization formally adds only one electron to the valence shell of each metal, the bonding electrons of the amido and imido ligands can be more effectively utilized because of greater overlap with hybrid metal orbitals generated in the lower symmetry (vide infra).³⁵ In $[(^t\text{Bu}_3\text{SiNH})\text{Ti}]_2(\mu\text{-NSi}^t\text{Bu}_3)_2$ (**17**), the asymmetric $\mu\text{-NSi}^t\text{Bu}_3$ bridges essentially draw the titanium centers close together while maximizing bridge bonding.

Steric factors also play a critical role in determining the geometry of the complex. The approximate center of a crude tetrahedron composed of the four nitrogens is roughly 2.1 Å from each. In this sense, the amide and μ -imide ligands are sterically situated as if they were binding to a single metal, rather than the dititanium unit. Similarly, a nearly regular tetrahedron is generated by the four silicon atoms. Figure 3 depicts the interconversion of two resonance structures, I and I', via a symmetric C_{2v} geometry, II. A minor steric barrier would be associated with these bond shifts, since only a slight reorientation of the $^t\text{Bu}_3\text{Si}$ moieties should accompany such a transformation, which is rem-

(40) (a) Vasyutinskaya, E. A.; Yermenko, I. L.; Nefedov, C. E.; Katugin, A. C.; Pasynskii, A. A.; Slovokhotov, Yu. L.; Strychov, Yu. L. *Metalloorg. Khim.* **1989**, *2*, 934–936. For a similar dichromium complex (e.g., $[\text{CpCr}=\text{NSiMe}_3]_2(\mu\text{-NSiMe}_3)_2$, $d(\text{Cr}–\text{Cr}) = 2.569$ (4) Å), see: (b) Wiberg, H.; Häring, H.-W.; Schubert, U. *Z. Naturforsch.* **1978**, *33B*, 1365–1369.

incent of the low-energy $C_{2h} \rightarrow D_{2h} \rightarrow C_{2h}$ tetrahedral equilibration in $W_4(O^iPr)_{12}$.⁴¹

The asymmetry manifested by the μ -NSi^tBu₃ ligands is not sterically induced, because the ^tBu₃Si groups are symmetrically disposed about the dititanium unit. Examination of the top view (B) in Figure 2 reveals that the Ti₂N₄ core appears twisted relative to the silicon positions, resulting in molecular C₂ symmetry rather than C_{2v}. The differences in the bridge bonds and angles manifest greater π -bonding in Ti1–N2 and Ti2–N1 than their counterparts. The short imido distances (i.e., Ti1–N2, Ti2–N1) of 1.940 (3)_{av} Å supplement the Ti1–N2–Si2 and Ti2–N1–Si1 angles of 155.6 (9)_{av}°, while the longer Ti1–N1 and Ti2–N2 bonds (1.992 (3)_{av} Å) are in concert with the Ti1–N1–Si1 and Ti2–N2–Si2 angles of 125.04 (4)_{av}°. Although this disparity is clear, the 1.966 (2)_{av} Å titanium–amide bonds (i.e., Ti1–N4, Ti2–N3) are nearly equal to the short imido distances, indicating similar π -bonding. Since even the longer of the two imido bridge distances is quite short, the μ -imido p π -orbital donates to both metal centers, albeit inequitably. As expected for the smaller first-row element, the Ti–NHR distances are shorter than previously characterized Zr complexes: (^tBu₃SiNH)₃ZrMe, $d(Zr-N) = 2.039$ (6)_{av} Å, $\angle(Zr-N-Si) = 151.3$ (8)_{av}°;¹⁰ (^tBu₃SiNH)₂(THF)Zr=NSi^tBu₃, $d(Zr-N_{am}) = 2.028$ (6)_{av} Å, $\angle(Zr-N-Si) = 157$ (2)_{av}°.¹¹ Terminal phenylamido¹⁹ and μ -phenylimido³⁸ bonds are ~ 0.05 Å shorter than those of 17. The Ti–N–Si angles of the amides (142.9 (6)_{av}°) are somewhat smaller than those of the Zr complexes, presumably due to reduced steric interactions in the dinuclear complex.

EHMO Calculations on [(^tBu₃SiNH)Ti]₂(μ -NSi^tBu₃)₂ (17). In order to identify electronic factors responsible for the short Ti–Ti bond, and the unusual exo disposition of the titanium atoms relative to their respective μ -imido and amido nitrogens, extended Hückel molecular orbital (EHMO) calculations of [(^tBu₃SiNH)Ti]₂(μ -NSi^tBu₃)₂ (17) were undertaken. The unusual pyramidalization at Ti was initially addressed by calculating the total energy of hypothetical [(H₃Si)HNTi]₂(μ -NSiH₃)₂ (17'), modeling 17, as a function of both Ti–Ti–NH(SiH₃) angles, each defined as θ ($90^\circ \leq \theta \leq 190^\circ$). The calculations revealed a minimum at 123° that roughly corresponds to the observed $\theta = 112^\circ$, but the potential energy curve, shown in Figure 4, was very flat from 112 to 142° with a gradual increase toward higher θ . A minimum at 120° and a similar flat potential energy curve was obtained when all SiH₃ groups were replaced by H (i.e., [H₂NTi]₂(μ -NH)₂ (17'')). Marginally excluded on this basis is a geometry composed of coplanar Ti, μ -N, and amide units (i.e., trigonal planar about Ti), which would require a θ of $\sim 157^\circ$. A structure sterically similar to 17', in which the amide NH group is rotated 180° about the Ti–Si interatomic vector, cannot be convincingly eliminated on the basis of the calculations, since θ is $\sim 136^\circ$.

Rotation of the Ti–amide bond was examined in similar fashion, but the observed geometry in which the amide substituents are effectively in the Ti₂N(amide)₂ plane (i.e., substituents in the xz plane, $\phi = 0^\circ$; for 17, $\phi = 4^\circ$) was not reproduced. Maximization of π -bonding occurred at $\phi \sim 90^\circ$ and 270° , suggesting that the steric requirements of the ^tBu₃Si groups play the major role in establishing the Ti–N(amide) torsional angle. This contention was corroborated by calculations of $E(\theta)$ for models where the NH(SiH₃) group was replaced by NH₂, NH₃ (charge adjusted to retain the same d-electron count), or H. In each instance, the general features of Figure 4 were repeated; thus when $\phi \sim 0^\circ$, amide π -bonding is not considered an important factor in determining the geometry of 17. Further scrutiny of the amide p π -orbitals revealed that individual interactions with Ti₂(μ -imido)₂ fragment orbitals were minor, in accord with the $E(\theta)$ results. Replacement of the bridging μ -NSiH₃ by μ -NH had little effect, but substitution with a μ -H ligand caused substantial changes; hence π -bonding by the bridging imide is essential.

Figure 5 depicts a truncated molecular orbital diagram for [H₂NTi]₂(μ -NH)₂ (17''), chosen as the model for simplicity and

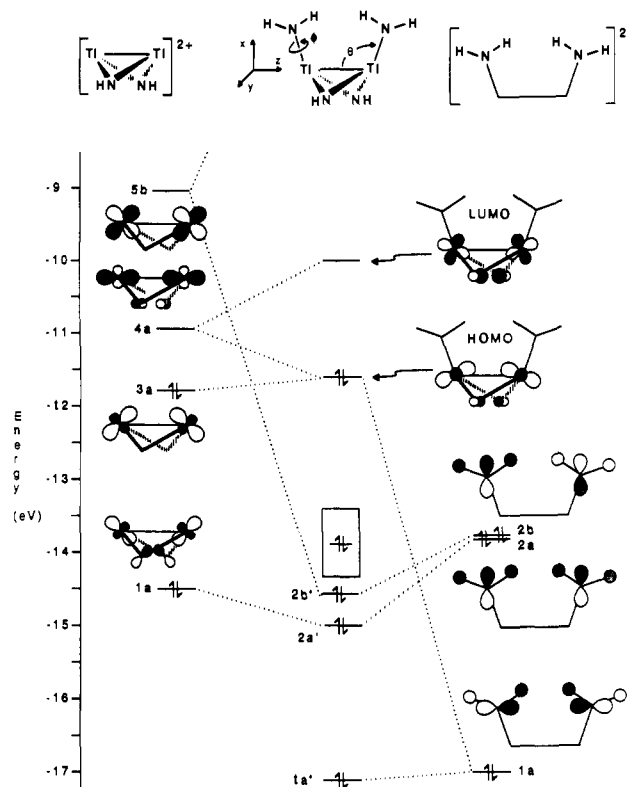


Figure 5. Truncated molecular orbital diagram of [(H₂N)Ti]₂(μ -NH)₂ (17''), a model complex of [(^tBu₃SiNH)Ti]₂(μ -NSi^tBu₃)₂ (17).

convenience. Orbitals pertinent to a discussion of the dimer's pyramidal geometry are illustrated; most antibonding orbitals and the majority of those involved in Ti–N bonding have been removed for the sake of clarity. The HOMO and HOMO–LUMO gap energies for 17'' compared favorably with those of 17' when calculated as a function of θ , thus use of the simpler model was considered legitimate. At $\theta = 112^\circ$, the HOMO–LUMO gap is an ample 1.54 eV, thereby accounting for the observed diamagnetism. Although the LUMO was influenced by the Si substituents, the added interactions were not considered germane to the Ti₂N₄ core, since only minor geometry changes were detected.

Due to the low symmetry of the complex, the bonding is not easy to analyze, even for the simplified model (17'': $\theta = 112^\circ$, $\phi = 0^\circ$). For example, it is unrealistic to describe the Ti–Ti interaction as a σ - or π -bond, because of the multicomponent nature of the critical orbitals. In this case, the HOMO, which contributes 0.247 of the 0.379 total Ti–Ti overlap population, is composed of approximately 3% s (σ), 20% d_{z²} (σ), 16% d_{xz} (π), and 9% d_{x²-y²} (δ) character per titanium. As a consequence of this mixing, a major portion of the electron density comprising the metal–metal bond does not reside along the Ti–Ti vector, but somewhat to the side of the amido ligands.⁴² The LUMO, another titanium–titanium bonding orbital, possesses substantial amplitude on the underside of the Ti–Ti vector as a consequence of the $\sim 18\%$ imido p-character of the orbital. Each titanium contributes 5% s (σ), 23% d_{z²} (σ), and 13% d_{xz} (π); hence the LUMO has greater σ -character, yet retains a considerable π -component. From calculations of $E(\text{HOMO})$ vs θ , minimization of its orbital energy occurs at $\sim 140^\circ$; hence other factors, such as lower lying Ti–N bonding orbitals, must contribute crucially in establishing the exo constitution of the titanium atoms.

The "upright" orientation of the amido groups, and thus the pyramidalization at titanium, is the result of a complicated set of subtle interactions. In Figure 5, the molecular orbital diagram corresponding to [H₂NTi]₂(μ -NH)₂ (17'') is described via the

(41) Chisholm, M. H.; Clark, D. L.; Hampden-Smith, M. J. *J. Am. Chem. Soc.* **1989**, *111*, 574–586.

(42) For a brief discussion regarding orbital orientation effects on metal–metal distances, see: Ferguson, G. S.; Wolczanski, P. T.; Párkányi, L.; Zonneville, M. C. *Organometallics* **1988**, *7*, 1967–1979.

confluence of the fragment molecular orbitals of $[\text{Ti}]_2(\mu\text{-NH})_2$ and $[\text{H}_2\text{N}]_2$. At $\theta = 112^\circ$, the interaction of $[\text{H}_2\text{N}]_2$ 1a with $[\text{Ti}]_2(\mu\text{-NH})_2$ 1a is negligible, yet it does interact with 3a and 4a to a small extent, despite having an unfavorable energy match. In contrast, 2a of $[\text{H}_2\text{N}]_2$ interacts with $[\text{Ti}]_2(\mu\text{-NH})_2$ 1a quite strongly. As θ is increased, the situations reverse; the mixing of $[\text{Ti}]_2(\mu\text{-NH})_2$ 1a with $[\text{H}_2\text{N}]_2$ 1a is turned on at the expense of the $[\text{H}_2\text{N}]_2$ 2a interaction, which now mixes with 3a. In the latter event, the HOMO is driven significantly higher in energy as θ increases, despite further mixing with 4a, and the overall total energy undergoes a minor increase. One can see this effect by comparing the 3a and HOMO orbital depictions; 3a mixing with 1a of $[\text{H}_2\text{N}]_2$ reorients the metal orbital components for maximum Ti-Ti overlap, whereas interaction with 2a actually directs these orbitals away from one another. Of secondary importance is the involvement of $[\text{Ti}]_2(\mu\text{-NH})_2$ 5b with $[\text{H}_2\text{N}]_2$ 2b, which also favors a θ of less than 157° (i.e., trigonal planar about Ti). Since the interactions that occur when θ is varied are interrelated, the soft potential energy surface illustrated in Figure 4 can be easily rationalized.

The interactions that determine the asymmetry of the imido bridges are also quite complex, and many of the orbitals involved are not illustrated in Figure 5, but constitute several of those indicated by the box. Essentially, the arguments follow the second-order Jahn-Teller distortion arguments originally postulated by Thorn et al.³⁵ for asymmetric $[\text{Me}_2(\text{t}^i\text{BuN})\text{W}]_2(\mu\text{-N}^i\text{t}^i\text{Bu})_2$ vs symmetric $[(\text{Me}_2\text{N})_2\text{Ti}]_2(\mu\text{-N}^i\text{t}^i\text{Bu})_2$. The same amide interactions that are involved in the pyramidalization at titanium encourage asymmetrization of the imido bridges, permitting greater orbital mixing and stability in the lower (C_2 vs C_{2v}) symmetry.

In summary, the pyramidalization at Ti maximizes the overlap necessary for metal-metal bonding, strengthens the asymmetric bridge bonding, and tends to minimize Ti-N(amide) antibonding interactions, but the effects are extremely subtle. The short Ti-Ti bond arises from two factors. Most importantly, the asymmetric imido bridges require a close approach of the titanium centers, as previously addressed. Second, the titanium-based fragment orbitals are not oriented directly toward one another (e.g., 3a); consequently, the maximum metal-metal overlap occurs at distances shorter than typical single bonds.⁴²

Concluding Remarks

Various monomeric, terminal imido complexes of titanium have been prepared via thermolyses that induce the abstraction of amide protons by neighboring HNSi^iBu_3 groups. Two important factors mitigate against the dimerization to form μ -imido species. The substantial bulk of the tri-*tert*-butylsilyl moieties, in concert with the relatively small covalent radius of Ti, renders dimerization sterically unfavorable. Electronic saturation is supplied by the substantial π -donating capacity of the imido and remaining ligands, with the exception of the alkyls. Each new four-coordinate species can be considered at least a $16e^-$ complex, provided every ligand donates the maximum number of π -bonding electrons.

The ^1H NMR spectra of these molecules may provide an interesting measure of the relative electrophilicity of the titanium centers. Assume that the chemical shift of an amido proton reflects the amount of π -donation from the corresponding nitrogen. Since the chemical shift of the $^i\text{Bu}_3\text{SiNH}_3^+$ is δ 8.37 (benzene- d_6),²¹ a downfield shift of the amido resonance should correlate with greater $^i\text{Bu}_3\text{SiN}(\text{H})=\text{Ti}$ character, indicating a more electrophilic titanium center. As indicated in Table I, the amido chemical shifts span a range of nearly 4 ppm, with $(^i\text{Bu}_3\text{SiNH})(\text{THF})\text{ClTi}=\text{NSi}^i\text{Bu}_3$ (9) displaying its resonance at δ 9.40 and $(^i\text{Bu}_3\text{SiNH})_2(\text{THF})\text{Ti}=\text{NSi}^i\text{Bu}_3$ (13) at δ 5.48. This major dissimilarity must arise from the fact that the silamide is both a greater σ - and π -donor to titanium than chloride. Differentiation between σ - and π -effects cannot be made by this chemical shift criterion, and each appears to be significant. For example, note that the Me and ^iBu ligands of $(^i\text{Bu}_3\text{SiNH})(\text{THF})\text{RTi}=\text{NSi}^i\text{Bu}_3$ ($\text{R} = \text{Me}$, δ 7.35 (15); ^iBu , δ 6.11 (16)) donate more electron density to the metal center in comparison to Cl, despite a lack

of π -orbitals, but less so than the silamide. Further inspection of Table I leads to the following tentative order of relative σ - and π -donation to titanium: $^i\text{Bu}_3\text{SiN} > ^i\text{Bu}_3\text{SiNH} > ^i\text{Bu} > \text{Me} > \text{OR}_2 > \text{Cl} > \text{Br}$.

One intriguing facet to the structure of $(^i\text{Bu}_3\text{SiNH})\text{Ti}_2(\mu\text{-NSi}^i\text{Bu}_3)_2$ (17) concerns its relationship to group 14 congeners. The dimer is isolobal⁴³ with a diazabicyclobutane and by inference related to bicyclo[$n.n.0$]alkanes ($n \geq 1$)⁴⁴ and propellanes.⁴⁵⁻⁴⁷ For bicyclo[1.1.0]butanes, the most strained of the bicyclic molecules,⁴⁷ two geometric features are particularly interesting in comparison to 17. Similar to the dimer's amido groups, bicyclo[1.1.0]butane bridgehead substituents are somewhat "upright" with respect to the bridgehead-bridgehead (C_b-C_b) bond (i.e., $\angle\text{C}_b\text{C}_b\text{H} = 128.4^\circ$ in C_4H_6),⁴⁸ although substantial variation in the $\text{C}_b\text{C}_b\text{R}$ angle has been observed.⁴⁹ In addition, relatively short C_b-C_b bond distances are often discerned in comparison to the neighboring cyclopropane C_b-CR_2 bond lengths.⁴⁹ These observations may be construed as manifestations of a bent C_b-C_b bond, much in the same vein as the aforementioned Ti-Ti linkage in 17. As the $\text{C}_b\text{C}_b\text{R}$ angle becomes smaller in a bicyclo[1.1.0]butane, less antibonding character is mixed into orbitals used in C_b-C_b bonding. The pyramidalization of the titanium atoms in 17 reflects a similar influence of the "upright" amido groups on the intermetallic interaction.

The comparison of $(^i\text{Bu}_3\text{SiNH})\text{Ti}_2(\mu\text{-NSi}^i\text{Bu}_3)_2$ (17) may be extended to include propellanes,⁴⁵⁻⁴⁷ since the terminal amides in 17 are approaching one another. The [1.1.1]propellanes have an extremely strong C_b-C_b bond (~ 65 kcal/mol)⁴⁵ that is characterized by a high charge density region central to the bridgehead carbons,⁴⁶ but a rather diffuse bond.⁵⁰ A parallel can be made with the rather diffuse character of the Ti-Ti bond in 17, as evidenced by the varied composition of the HOMO. The propellane family was recently expanded to include a derivatized pentastannane[1.1.1] complex, prepared by Sita,⁵¹ in which the long Sn_b-Sn_b interaction is best described as an extremely weak bond or a singlet diradical.⁵² It would be interesting to generate group 4 analogues of these species in order to study the corresponding metal-metal interaction.

The ready formation of $(^i\text{Bu}_3\text{SiNH})\text{Ti}_2(\mu\text{-NSi}^i\text{Bu}_3)_2$ (17) upon hydrogenation of $(^i\text{Bu}_3\text{SiNH})(\text{THF})\text{RTi}=\text{NSi}^i\text{Bu}_3$ ($\text{R} = \text{Me}$ (15); ^iBu (16)) remains somewhat of a curiosity. According to Scheme II, the putative hydride, $(^i\text{Bu}_3\text{SiNH})(\text{THF})\text{HTi}=\text{NSi}^i\text{Bu}_3$ (18), is unstable relative to loss of dihydrogen and dimerization with concomitant THF loss, underscoring a previously noted instability of titanium(IV) hydrides.^{53,54} While the inherent stability of the lower oxidation state (i.e., Ti(III) of 17) must be the underlying factor in determining the thermodynamics of this reaction, the rapid formation of 17 may signify a radical chain process in which Ti(III) species play prominent roles.² Presum-

(43) Hoffmann, R. *Angew. Chem., Int. Ed. Engl.* **1982**, *21*, 711-724.

(44) Dowd, P.; Irngartinger, H. *Chem. Rev.* **1989**, *89*, 985-996, and references therein.

(45) (a) Wiberg, K. B. *Chem. Rev.* **1989**, *89*, 975-983. (b) Wiberg, K. B. *Acc. Chem. Res.* **1985**, *17*, 379-386, and references therein.

(46) Wiberg, K. B.; Bader, R. F. W.; Lau, C. D. H. *J. Am. Chem. Soc.* **1987**, *109*, 985-1001.

(47) Wiberg, K. B.; Bader, R. F. W.; Lau, C. D. H. *J. Am. Chem. Soc.* **1987**, *109*, 1001-1012.

(48) Cox, K. W.; Harmony, M. D.; Nelson, G.; Wiberg, K. B. *J. Chem. Phys.* **1969**, *50*, 1976-1980; **1970**, *53*, 858.

(49) For a pertinent review, see: Eisenstein, M.; Hirshfeld *Acta Crystallogr.* **1983**, *B39*, 61-75.

(50) The nature of this interaction has been under contention. For other theoretical and experimental characterizations, see: (a) Allen, L. C.; Jackson, J. E. *J. Am. Chem. Soc.* **1984**, *106*, 591-599. (b) Seiler, P.; Belzner, J.; Bunz, U.; Szeimies, G. *Helv. Chim. Acta* **1988**, *71*, 2100-2110.

(51) (a) Sita, L. R.; Bickerstaff, R. D. *J. Am. Chem. Soc.* **1989**, *111*, 6454-6456. For comparison, see: (b) Sita, L. R.; Bickerstaff, R. D. *J. Am. Chem. Soc.* **1989**, *111*, 3769-3770.

(52) Nagase, S.; Kudo, T. *Organometallics* **1987**, *6*, 2456-2458.

(53) (a) Bercauw, J. E. *J. Am. Chem. Soc.* **1974**, *96*, 5087-5095. (b) Bercauw, J. E.; Marvich, R. H.; Bell, L. G.; Brintzinger, H. H. *J. Am. Chem. Soc.* **1972**, *94*, 1219-1238. (c) Bercauw, J. E.; Brintzinger, H. H. *J. Am. Chem. Soc.* **1969**, *91*, 7301-7306.

(54) Aitken, C. T.; Harrod, J. F.; Samuel, E. J. *J. Am. Chem. Soc.* **1986**, *108*, 4059-4066.

ably, the swift dinuclear elimination of H₂ to give **17** also reflects the ease of dihydrogen reductive elimination due to the spherical nature of the hydride-localized orbitals.⁵⁵ Related thermodynamic arguments suggest that 2 equiv of (t-Bu₃SiNH)(THF)RTi=NSi^tBu₃ (R = Me (**15**); t-Bu (**16**)) should also be unstable with respect to **17** and R₂. Fortunately, the dimerization of either alkyl derivative may be sterically prohibitive, especially where R = t-Bu, and the dinuclear reductive elimination of R₂ suffers from intrinsic difficulties regarding the directionality of the sp³-orbitals of the R groups.⁵⁵ Further synthetic efforts and reactivity studies of the imido complexes and **17** are ongoing.

Experimental Section

General Considerations. All manipulations were performed with either glovebox or high vacuum line techniques. Hydrocarbon solvents containing 1–2 mL of added tetraglyme were distilled under nitrogen from purple benzophenone ketyl and vacuum transferred from same prior to use. Benzene-d₆ and cyclohexane-d₁₂ were dried over activated 4-Å molecular sieves, vacuum transferred, and stored under N₂; THF-d₈ was dried over sodium benzophenone ketyl. All glassware was oven-dried, and NMR tubes were additionally flamed under dynamic vacuum. Dihydrogen was passed over MnO on vermiculite and activated 4-Å molecular sieves,⁵⁶ and t-Bu₃SiNHLi¹⁰ was prepared from t-Bu₃SiNH₂²¹ according to published procedures.

NMR spectra were obtained by using Varian XL-200 and XL-400 spectrometers. Infrared spectra were recorded on a Mattson FT-IR interfaced to an AT&T/PC7300 computer. Analyses were performed by Analytische Laboratorien, Elbach, West Germany, or Oneida Research Services, Whitesboro, New York.

Procedures. **1.** (t-Bu₃SiNH)₃TiCl (**1**). To a flask containing a solution of t-Bu₃SiNHLi (5.00 g, 22.6 mmol) in 125 mL of ether at 0 °C was added solid Cl₄Ti(THF)₂ (2.51 g, 7.52 mmol) in small portions over 5 h. The reaction mixture was allowed to stir for an additional 4 h at 25 °C, at which time the volatiles were removed under vacuum. Exhaustive extraction and filtration with 75-mL portions of pentane followed by concentration of the combined extracts to ~60 mL gave a slurry of microcrystalline (t-Bu₃SiNH)₃TiCl (**1**). The slurry was cooled to 0 °C and stirred for 1 h, and the colorless product was isolated by filtration and dried under vacuum (4.50 g, 82%). IR (Nujol, cm⁻¹) 3247 (w, NH), 3237 (w, NH), 1386 (m), 1365 (m), 1064 (s, br), 1011 (m), 1003 (m), 932 (m), 869 (w), 826 (s, sh), 818 (s), 794 (s, br), 621 (m), 608 (w). Anal. Calcd for TiSi₃ClN₃C₃₆H₅₄: C, 59.50; H, 11.65; N, 5.78. Found: C, 59.99; H, 11.42; N, 5.57.

2. (t-Bu₃SiNH)₃TiBr (**2**). To a flask containing (t-Bu₃SiNH)₃TiCl (**1**; 510 mg, 0.70 mmol) and MgBr₂ (1.00 g, 5.4 mmol) was distilled 25 mL of THF by vacuum transfer. The solution was allowed to stir for 12 h at 25 °C and solvent removed under vacuum. Exhaustive extraction and filtration of the residue with 20 mL of hexanes followed by removal of volatiles gave a residue containing ca. 20% **1**. The procedure was repeated with 1.00 g of MgBr₂ in 25 mL of THF (12 h, 25 °C), and again with 0.50 g of MgBr₂ in 10 mL of THF (1 h, 25 °C). The final extracts were reduced to 5 mL and the slurry was stirred for 1 h at 0 °C before the product was collected by filtration as a white powder (221 mg, 0.29 mmol, 41%). According to ¹H NMR, <1% of **1** remained. IR (Nujol, cm⁻¹) 3242 (w, NH), 3237 (w, NH), 1386 (m), 1365 (m), 1064 (s, br), 1013 (m), 1004 (w), 954 (w), 922 (m, sh), 934 (m), 869 (m, br), 837 (s), 795 (s, br), 621 (m), 589 (m). Anal. Calcd for C₃₆H₅₄N₃BrSi₃Ti: C, 56.07; H, 10.98; N, 5.45. Found: C, 55.89; H, 11.62; N, 5.27.

3. (t-Bu₃SiNH)₂(Et₂O)Ti=NSi^tBu₃ (**4**). To a flask containing a solution of (t-Bu₃SiNH)₃TiCl (**1**; 400 mg, 0.55 mmol) in ether (10 mL) was added 0.4 mL of MeLi (1.4 M in Et₂O) under Ar counterflow at -78 °C. The solution was allowed to warm to 25 °C and stirred for 12 h. The volatiles were removed, and the solid was extracted with 20 mL of hexanes followed by concentration to ~10 mL. Upon cooling to -78 °C, 280 mg (~55%) of white microcrystals were collected by filtration. The ¹H NMR indicated a persistent, unidentified impurity present in ~10%; thus no analysis was attempted. IR (Nujol, cm⁻¹) 3241 (w, NH), 1657 (w), 1363 (m), 1286 (w), 1189 (m), 1149 (m), 1089 (m), 1059 (s, br), 1011 (m), 994 (m), 964 (s), 932 (m), 886 (m), 848 (s), 819 (s, br), 778 (m), 614 (s), 470 (w).

4. (t-Bu₃SiNH)(THF)CITi=NSi^tBu₃ (**9**). To a glass bomb reactor containing (t-Bu₃SiNH)₃TiCl (**1**; 1.67 g, 2.30 mmol) was added ~50 mL of THF via vacuum transfer. The reactor was immersed in a wax bath at 120 °C for 14 h, during which time the colorless solution became pale yellow. The THF solution was filtered and the volatiles were removed

under vacuum. The resulting yellow solid was triturated once in 25 mL of hexanes, slurried in pentane at 0 °C for 1 h, and collected by filtration. Drying under vacuum provided **9** as a pale yellow powder (1.12 g, 83%). IR (Nujol, cm⁻¹) 3298 (w, NH), 1340 (w), 1112 (s, br), 1023 (m), 1011 (m), 1000 (m), 931 (m, br), 920 (w), 862 (m, sh), 848 (s), 815 (s), 617 (m), 602 (w). Anal. Calcd for C₂₈H₄₃N₃O₂Si₃Ti: C, 57.65; H, 10.89; N, 4.80. Found: C, 58.44; H, 10.63; N, 4.52.

5. (t-Bu₃SiNH)(THF)BrTi=NSi^tBu₃ (**11**). A solution of 4% by volume THF in C₆D₆ containing 21 mg (0.034 mmol) of (t-Bu₃SiNH)₃TiBr (**2**) was introduced into a 5-mm flame-dried NMR tube sealed to a 14/20 joint. The tube was attached to a 180° needle valve, freeze-pump-thaw degassed three times (77 K), and flame-sealed. Thermolysis at 81.4 °C for 10 h (*k* = 0.97 (2) × 10⁻⁴ s⁻¹) gave a yellow solution of **11** in >95% yield by ¹H NMR.

6. (t-Bu₃SiNH)₄Ti (**12**). To a flask containing (t-Bu₃SiNH)₃TiCl (**1**; 1.12 g, 1.54 mmol) and t-Bu₃SiNHLi (346 mg, 1.54 mmol) was distilled 25 mL of benzene by vacuum transfer. The reaction mixture was refluxed for 3 days before cooling, and the volatiles were removed under vacuum. The residue was extracted with hexanes (4 × 10 mL), concentrated to 6–7 mL, and stirred for 1 h at -78 °C before **12** was collected by filtration as a pale yellow powder (820 mg, 907 mmol, 59%). IR (Nujol, cm⁻¹) 3222 (w, NH), 1365 (m), 1075 (s, br), 1013 (m), 1008 (w), 936 (m), 822 (s), 780 (s, br), 723 (m), 621 (m). Anal. Calcd for C₄₈H₁₁₂N₄Si₄Ti: C, 63.03; H, 12.48; N, 6.19. Found: C, 63.37; H, 12.40; N, 5.62.

7. (t-Bu₃SiNH)₂(THF)Ti=NSi^tBu₃ (**13**). To a flask containing (t-Bu₃SiNH)₃Ti (**12**; 0.697 g, 0.770 mmol) was distilled 25 mL of THF by vacuum transfer. The solution was refluxed for 12 h. Upon removal of the volatiles, the residue was dissolved in 10 mL of pentane and filtered. The solid was extracted three times with 5 mL of pentane, concentrated to 5 mL, and stirred at -78 °C for 1 h before filtering to obtain a white powder (330 mg, 53%). IR (Nujol, cm⁻¹) 3268 (w, NH), 3242 (w, NH), 1364 (m), 1191 (w), 1106 (w), 1089 (m), 1057 (s), 1011 (m), 932 (m), 877 (m), 847 (s), 814 (s, br), 612 (m), 583 (m). Anal. Calcd for C₄₀H₉₁N₃O₂Si₃Ti: C, 63.02; H, 12.03; N, 5.51. Found: C, 63.28; H, 10.88; N, 5.29.

8. (t-Bu₃SiNH)(THF)MeTi=NSi^tBu₃ (**15**). To a flask containing (t-Bu₃SiNH)(THF)CITi=NSi^tBu₃ (**9**; 0.900 g, 1.542 mmol) was distilled 15 mL of ether by vacuum transfer. MeLi (1.1 equiv, 1.2 mL of 1.4 M solution in Et₂O) was syringed in under argon counterflow at -78 °C. The resulting clear, colorless solution was stirred for 0.5 h at -18 °C before the volatiles were removed. The residue was taken up in 10 mL of hexanes and filtered, leaving a white solid that was extracted (5 × 10 mL) with hexanes. The solution was concentrated to 5 mL, cooled to -78 °C for 0.5 h, and filtered to obtain an off-white, microcrystalline solid. This solid was repeatedly triturated in hexanes (7 × 20 mL) for 15 min at 25 °C. The final yellow-brown solution was concentrated to 5 mL and filtered at -78 °C to yield off-white microcrystals (405 mg, 47%); a second crop was obtained (73 mg, 55% total). IR (Nujol, cm⁻¹) 3280 (w, NH), 1114 (s), 1089 (m), 1023 (m, br), 1008 (m), 1004 (m, sh), 994 (m, sh), 928 (m, br), 863 (m), 848 (s), 811 (s), 611 (s). Anal. Calcd for C₂₉H₆₆N₂O₂Si₃Ti: C, 61.87; H, 11.81; N, 4.98. Found: C, 60.34; H, 11.20; N, 4.75.

9. (t-Bu₃SiNH)(THF)^tBuTi=NSi^tBu₃ (**16**). To a flask containing (t-Bu₃SiNH)(THF)CITi=NSi^tBu₃ (**9**; 1.46 g, 2.50 mmol) in 30 mL of ether at -78 °C was added solid t-BuLi (0.16 g, 2.50 mmol) in small portions over a 10-min period. The resulting bright yellow solution was stirred at -78 °C for 40 min and then warmed to 25 °C over 20 min, followed by a 15-min period at 25 °C. All volatiles were removed under vacuum. The yellow residue was triturated repeatedly in hexanes (4 × 25 mL) to remove all excess ether. This process apparently precludes formation of chloride adducts, which precipitate LiCl on dissolution in benzene. The material was next extracted with pentane (4 × 20 mL) and filtered, and the combined extracts were concentrated to ~12 mL and slurried for 1 h at 0 °C. Filtration and vacuum drying yielded **16** (1.15 g, 76%) as a thermally unstable yellow powder (*t*_{1/2} ~ 48 h (0.05 M in benzene)) that was stored at -20 °C. IR (Nujol, cm⁻¹) 1089 (s), 1055 (m), 1011 (m), 1006 (m), 930 (m), 860 (m, sh), 848 (s, br), 816 (s), 792 (w), 735 (m, sh), 723 (m), 614 (m), 597 (w).

10. a. Synthesis of [(t-Bu₃SiNH)Ti]₂(μ-NSi^tBu₃)₂ (17**).** To a 30-mL glass bomb containing (t-Bu₃SiNH)(THF)^tBuTi=NSi^tBu₃ (**16**; 0.76 g, 1.25 mmol) was added 10 mL of benzene via vacuum transfer. The bomb was immersed in liquid nitrogen, 0.9 atm H₂ added, and the vessel allowed to warm to 25 °C. Immersion of the bomb reactor in a 65 °C water bath elicited a color change from yellow to orange-red in less than 1 min. The solution was maintained at 65 °C for 3 h and allowed to cool to 25 °C; the volatiles were removed and the red solid residue was filtered in hexanes (10 mL). Cooling and concentration of the solution gave red crystals that were isolated by filtration at -78 °C (290 mg). A second crop was obtained similarly by filtration and crystallization from ether,

(55) Trinquier, G.; Hoffmann, R. *Organometallics* **1984**, *3*, 370–380.

(56) Brown, T. L.; Dickerhoff, D. W.; Bafus, D. A.; Morgan, G. L. *Rev. Sci. Instrum.* **1962**, *33*, 491.

from which the complex separates more easily (70 mg, total 61%). IR (Nujol, cm^{-1}) 1019 (m, br), 964 (m, br), 917 (m), 839 (s), 814 (s), 820 (s), 617 (m). Anal. Calcd for $\text{C}_{48}\text{H}_{110}\text{N}_4\text{Si}_4\text{Ti}_2$: C, 60.59; H, 11.65; N, 5.89. Found: C, 60.52; H, 10.82; N, 3.09.

b. H_2 Uptake by Toepler Pump. Treatment as described above of $(^1\text{Bu}_3\text{SiNH})(\text{THF})^1\text{BuTi}=\text{NSi}^1\text{Bu}_3$ (**16**; 256 mg, 0.42 mmol) with H_2 (0.37 mmol, 0.88 equiv) resulted in the uptake of 0.47 equiv of H_2/Ti atom. The residual H_2 was measured by Toepler pump and burned completely when heated to 325 °C in a 20-min cycle over a copper oxide. Inspection of the crude $[(^1\text{Bu}_3\text{SiNH})\text{Ti}]_2(\mu\text{-NSi}^1\text{Bu}_3)_2$ (**17**) from this experiment by ^1H NMR revealed that it had formed in >97% yield (a minor impurity in the crude product is $(^1\text{Bu}_3\text{SiNH})_2(\text{THF})\text{Ti}=\text{NSi}^1\text{Bu}_3$ (**13**; <3%). Correcting for the latter, 0.48 equiv of H_2/Ti are consumed.

c. H_2/D_2 Scrambling by **17.** Two flame-dried, 5-mm NMR tubes on 14/20 joints were charged with solutions of dimer (19 mg, 0.020 mmol) in C_6D_6 (~0.3 mL). One control tube was attached to a 180° needle valve. Another was attached to a 50.4-mL gas bulb, which was attached to a 91.0-mL gas bulb. The solutions were both freeze-pump-thaw degassed two cycles (77 K). H_2 (0.9 atm, 1.9 mmol) was admitted to the 50.4-mL gas bulb, and D_2 (0.5 atm, 1.9 mmol) to the 91.0-mL gas bulb; the two gas bulbs were allowed to equilibrate for 15 min before exposing the NMR tube to the H_2/D_2 mixture. After 5 min at 77 K, the tube, estimated to contain ~50 equiv each of H_2 and D_2 , was flame-sealed. D_2 (0.75 atm, ~50 equiv) was admitted to the control NMR tube, which was cooled for 5 min at 77 K before being flame-sealed. ^1H NMR spectra of both tubes were taken immediately. The control tube (eight scans, no delay) showed a $^1\text{Bu}/\text{NH}$ integral ratio of 64:1 (this is typically observed and does not reflect deuteration). The mixed-label tube (300 scans, no delay, 15-min acquisition time) already showed a ratio of H_2 to HD of 8.0:1. Heating for 0.5 h at 60 °C brought the H_2/HD ratio down to 4.2:1; an additional hour of heating brought this to 2.4:1, representing a turnover number of 17 after 1.5 h. After 30 min at 60 °C, the control tube showed a $^1\text{Bu}/\text{NH}$ integral ratio of 63:1; after 1.5 h this had risen to 69:1 (~7% deuterated), thus H_2 addition across the imido bond is only a minor scrambling pathway. ^1H NMR spectra of H_2 and D_2 in C_6H_6 in flame-sealed NMR tubes (300 scans, no delay) revealed no HD present in the initial gases.

General Kinetics. Solutions for kinetics were prepared in 2-mL volumetric flasks. Three samples were taken from each 2-mL solution. In cases where mixed $\text{C}_6\text{D}_6/\text{THF}-d_8$ was used, solvents were prepared by successive dilutions with C_6D_6 of a stock solution of $\text{C}_6\text{D}_6/\text{THF}-d_8$. Solutions were transferred to flame-dried, 5-mm NMR tubes sealed to 14/20 joints and attached to 180° needle valves. The tubes were freeze-pump-thaw degassed three cycles (77 K) and flame-sealed under vacuum. The three sample tubes were simultaneously heated by immersion in a poly(ethylene glycol) bath (average MW = 570–630) with a Polyscience Model 73 immersion circulator and were cooled quickly to ~20 °C in cold running water after removal from the bath. The bath temperatures were stable to ± 0.3 °C. Rates of disappearance of amido NH peaks were monitored in all cases except for the determination of $k(\text{NH})_3/k(\text{ND})_3$ (i.e., $(^1\text{Bu}_3\text{SiNH})_3\text{TiCl}$ (**1**) vs $(^1\text{Bu}_3\text{SiND})_3\text{TiCl}$ (**1-(ND)_3**)), which was followed by growth of liberated amine. All runs were monitored from 4 to 6 half-lives. Pulse delays of 15 s were used to obtain the most reproducible integrals. Rates and uncertainties were obtained by using weighted $(1/\sigma^2)$, where σ was obtained from three simultaneous runs, nonlinear least-squares fitting to the appropriate exponential form of each rate expression. Activation parameters were obtained from a weighted $(1/\sigma^2)$, where σ corresponds to Δk , the absolute

uncertainty in each rate constant), nonlinear fitting of the exponential form the Eyring equation (60.0–110.4 °C).

Single-Crystal X-ray Diffraction Analysis of $[(^1\text{Bu}_3\text{SiNH})\text{Ti}]_2(\mu\text{-NSi}^1\text{Bu}_3)_2\text{C}_6\text{H}_6$ (17-C}_6\text{H}_6).** A flat red needle ($0.2 \times 0.5 \times 0.6$ mm) of $[(^1\text{Bu}_3\text{SiNH})\text{Ti}]_2(\mu\text{-NSi}^1\text{Bu}_3)_2\text{C}_6\text{H}_6$ (**17-C}_6\text{H}_6), obtained from benzene solution, was sealed in a capillary. Preliminary X-ray diffraction photographs displayed monoclinic symmetry. Precise lattice constants, determined from a least-squares fit of 15 diffractometer-measured 2θ values at 25 °C, were $a = 12.033$ (3) Å, $b = 23.309$ (5) Å, $c = 22.741$ (4) Å, $\beta = 99.314$ (15)°. The cell volume was 6294 (2) Å³, with a calculated density of 1.087 g/cm³, where $Z = 4$. The space group was determined to be $P2_1/n$, and the antisymmetric unit consisted of $\text{C}_{54}\text{H}_{116}\text{N}_4\text{Si}_4\text{Ti}_2$. Diffraction maxima with $2\theta \leq 50^\circ$ were measured on a four-circle automated diffractometer (Nicolet R3m/V), with a variable-speed, 2θ - θ scan (3.00–15.00°/min in ω) using graphite-monochromated Mo K α radiation ($\lambda = 0.71069$ Å) at –80 °C. After correction for Lorentz, polarization, and background effects, 7806 (70.1%) of the unique data (11 129) were judged observed ($|F_o| \geq 4\sigma|F_o|$).⁵⁷ The structural solution proceeded using the SHELXL PLUS (VMS) system. The positions of all heavy atoms were deduced via direct methods. Full-matrix, least-squares refinements (minimization of $\sum w(F_o - F_c)^2$, where w ($w^{-1} = \sigma^2(F) + 0.0010F^2$) is based on counting statistics, modified by an ignorance factor) with anisotropic heavy atoms and all hydrogens included at calculated positions (Riding model, fixed isotropic U) have converged to $R = 6.64\%$ and $R_w = 7.75\%$ (7806 reflections).⁵⁸ No absorption correction was attempted ($\mu = 3.58$ cm⁻¹) and a final difference Fourier map revealed no peaks greater than 1.20 e⁻/Å³.****

Extended Hückel Molecular Orbital Calculations on $[(^1\text{Bu}_3\text{SiNH})\text{Ti}]_2(\mu\text{-NSi}^1\text{Bu}_3)_2$ (17**).** Calculations were done by the extended Hückel method.⁵⁹ The bond lengths and angles were taken from Table III. The parameters (atom, orbital, H_{ii} (eV), ζ_1 , ζ_2 , c_1^a , c_2^b) used were as follows: Ti, 4s, –8.97, 1.075; Ti, 4p, –5.44, 0.675; Ti, 3d, –10.80, 1.55, 1.40, 0.41853, 0.78542; N, 2s, –26.00, 1.95; N, 2p, –13.40, 1.95; Si, 3s, –17.30, 1.383; Si, 3p, –9.20, 1.383; C, 2s, –21.40, 1.625; C, 2p, –11.4, 1.625; H, 1s, –13.60, 1.3.

Acknowledgment. Support from the Air Force Office of Sponsored Research, the National Science Foundation, the NSF REU program (C.C.C.) and Cornell University is gratefully acknowledged. We also thank Profs. J. K. Burdett and B. K. Carpenter for helpful discussions, and the NIH and NSF instrumentation programs for support of the Cornell Nuclear Magnetic Resonance Facility.

Supplementary Material Available: Information pertaining to the X-ray structural investigation of $[(^1\text{Bu}_3\text{SiNH})\text{Ti}]_2(\mu\text{-NSi}^1\text{Bu}_3)_2\text{C}_6\text{H}_6$ (**17-C}_6\text{H}_6): a summary of crystal data encompassing data collection and solution/refinement, atomic coordinates, hydrogen atom coordinates, isotropic and anisotropic temperature factors, bond lengths, and bond angles (12 pages); observed and calculated structure factors (40 pages). Ordering information is given on any current masthead page.**

(57) Cromer, D. T.; Mann, J. B. *Acta Crystallogr., Sect. A* **1968**, *A24*, 321–324.

(58) $R = \sum ||F_o| - |F_c|| / (\sum |F_o|)$; $R_w = [\sum w(|F_o| - |F_c|)^2 / \sum w(|F_o|)^2]^{1/2}$.

(59) Hoffmann, R. *J. Chem. Phys.* **1963**, *39*, 1397–1412.